# A Comparative Analysis of Mould Growth on Exterior Sheathing of a Brick Masonry Wall in Different Canadian Climate Zones

by

Jasveer Singh

Bachelor of Technology in Mechanical Engineering

Guru Nanak Dev Engineering College, 2021

A Project Submitted in Partial Fulfillment of the

Requirements for the Degree of

MASTER OF ENGINEERING

in the Department of Mechanical Engineering



University of Victoria

# Supervisory Committee

## A Comparative Analysis of Mould Growth on Exterior Sheathing of a Brick Masonry Wall in Different Canadian Climate Zones

by

Jasveer Singh

Bachelor of Technology in Mechanical Engineering

Guru Nanak Dev Engineering College, 2021

**Supervisory Committee**

Dr. Phalguni Mukhopadhyaya, Department of Civil Engineering

Dr. Caterina Valeo, Department of Mechanical Engineering

# Abstract

This study investigates the risk of mould growth on sheathing boards in brick masonry walls in four Canadian cities: Vancouver, Ottawa, Calgary, and Saskatoon. The hygrothermal simulation tool WUFI® Pro 6.8 (1D) and the VTT Mold Index were used to conduct this investigation. The impact of moisture penetration through brick veneer cladding on the potential for mould growth in Oriented Strand Board (OSB), Fiberboard (FB), and Plywood (Ply) sheathing was assessed.

For hygrothermal simulations, a severe weather year was selected based on a 31-year historical weather dataset (1986-2016) using the severity index ($I_{sev}$) method prescribed in the ASHRAE Standard 160-2021. The calculation period was set for seven years, and two wall orientations were considered: (i) direction with the least solar radiation and (ii) maximum wind-driven rain direction. For each orientation, three rain penetration cases (1%, 2% and 3% of wind-driven rain) were considered, and two Air Change Rates (ACH 0 and ACH 15) were considered in the drainage cavity for each of the three rain penetration cases. As per ASHRAE 160-2021, the rain penetration was deposited on the outer layer of the water-resistive barrier (WRB).

The results showed that for the 1% rain penetration and no ventilation, the mould growth index (MGI) for all three sheathing boards remained at zero (i.e., No mould growth) for Vancouver's north-oriented wall (least solar radiation); however, the southeast-facing wall (maximum wind-driven rain) experienced a higher MGI (up to 5.3). For the same case (i.e. 1% rain penetration), the remaining simulated cities experienced MGI>5 (i.e., 50% visually covered surface). In the case of increased rain penetration and no ventilation, each sheathing board's mould growth performance significantly decreased (MGI>5) for all four cities in both orientations; however, an air change rate of 15/hour (ACH 15) in the drainage cavity reduced the mould growth (MGI<1, local growth microscopic level) in Calgary, Ottawa and Saskatoon. In contrast, ACH 15 was insufficient to reduce the MGI < 3 (i.e., visuals of mould <10% surface coverage) for the Vancouver location, except for the 1% rain penetration case.

# Table of Contents

# List of Tables

# List of Figures

# List of Equations

# Acknowledgment

I sincerely thank my supervisor, Dr. Phalguni Mukhopadhyaya. He has provided steadfast guidance, mentorship, and invaluable feedback throughout this endeavour. His expertise and encouragement have influenced my research direction and quality. Throughout my academic journey at the University of Victoria, he facilitated the development of my essential research and time management skills.

I am also profoundly grateful to Dr. Caterina Valeo for her insightful comments, constructive criticism, and unwavering support. Her contributions have greatly enhanced the refinement of my work.

Finally, I express my deep gratitude to my parents, family, and friends for their continuous support and encouragement throughout my academic journey and during the research and writing of this project. This achievement would not have been possible without their unwavering assistance.

## *Dedication*

***I dedicate this project to my beloved parents, sister, and family for their endless love and support.***

# Chapter 1: Research Overview

With the intensification of climate change, extreme rainfall events and prolonged humid conditions have risen globally, significantly heightening the risk of water damage to buildings.[1]. Annual winter precipitation is projected to increase all over Canada, while summer will bring low rainfall to the southern part of Canada[2]. Defo et al. highlighted the research needed to mitigate significant climate change challenges to building infrastructures, which affect the durability of materials and the comfort and health of occupants [3]. Taking action to mitigate climate change effects on Canadian buildings, the National Research Council Canada generated reliable historical and future predicted climate data to perform a hygrothermal analysis of the building envelope. Climate data for 564 locations were generated for which the data was considered from the 2020 version of Canadian Weather Energy and Engineering Datasets (CWEEDS)/Canadian Weather Year for Energy Calculation (CWEC) datasets from Environment and Climate Change Canada (ECCC) [4]. The methodology of the generated database is detailed in the paper published by Gaur et al. and available online for generating specific climate files for the hygrothermal software[2].

Weather effects are evaluated using hygrothermal simulation software. The hygrothermal design involves a comprehensive analysis to assess the wetting and drying of wall components within the building envelope, the moisture accumulation, and the risk of mould growth. [5]. These numerical simulations evaluate the effects of heat, air, and moisture transport within the building envelope. The long-period effect calculation is time-consuming. However, it can be minimized by selecting a set of years representing long-term severe climate data or Moisture Reference Years (MRY) to obtain similar results from the long-term simulations[6]. Numerous moisture indices, such as the Moisture Index[7], Climate Index [8], and Mould Growth Index [6], can rank the set of years to derive an MRY (worst year) or set of years representing various moisture severities, implementing ASHRAE 160-2021, ranking the years is based on severity index, and the analysis can be done by selecting a Moisture Reference Year or a set of ten consecutive years of weather data [9]

Wind-driven rain-induced moisture penetration through the building enclosure is a critical factor compromising the building envelope's durability and performance. It inevitably leads to many problems, such as fungal growth and damage to the interior building elements, such as cladding, sheathing boards, drywall, and insulation materials [10]. Typically, in low-rise buildings, the exterior cladding is regarded as the primary layer first affected by climatic conditions, and infiltered water or moisture will interact with the air in the drainage cavity and the water-resistive barrier (WRB) membrane, the secondary layer of protection (Refer to Figure 1) [11]. Sheathing boards are the structural components of the buildings and act as a third layer of defence. As water penetrates through the cladding materials, the sheathing board is at significant risk of mould growth as the wood is an organic material [12]. Mould generally occurs when favourable environmental conditions, with adequate relative humidity, temperature, nutrients, and oxygen [13]. As stated by the World Health Organization (WHO), the occurrence of visible mould and its spores poses significant human health risks [14]. The mould growth is particularly enhanced as moisture accumulates and the materials become saturated, leading to conditions suitable for high-humidity environments. Indoor dampness and elevated relative humidity levels, typically 70% to 80%, create conditions conducive to mould growth [15].

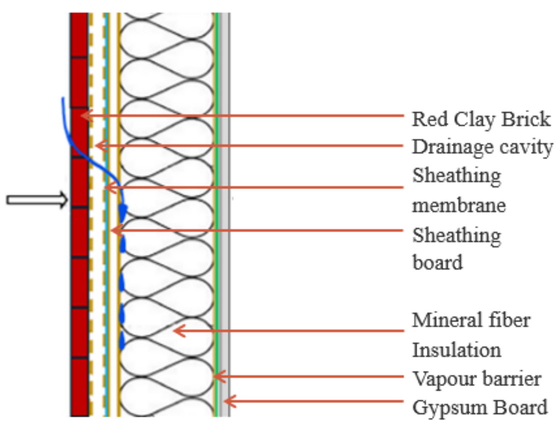


*Figure 1: Brick veneer wall assembly*

The Mould growth and moisture accumulation tests conducted in the laboratories and the recently published studies have concluded that the range of values for the incident rainfall can be deposited on the WRB or infiltrated through the first plane of protection. However, ASHRAE 160 recommends that the standard 1% fraction of rain load be sufficient for moisture design analysis[9].

The following sections of the report outline the recent research conducted to study the effect of climate change on building envelopes and the established standard to evaluate the effects of climate, specifically wind-driven rain penetration. Numerous studies have given many aspects to determine the fraction of infiltrated rain; however, the changing climatic conditions are getting extreme with global temperatures. The selected wall orientation is a standard brick veneer wall assembly that meets the National Building Code 2020 requirement to resist moisture damage in four different climates of Canadian cities: Vancouver, Calgary, Ottawa and Saskatoon. The climate files to perform the severe weather effect were generated from hourly weather data of 30 years and a moisture reference year (MRY) representing a severe year for moisture design detailed in the subsequent sections. The wall's performance was evaluated based on the Mould Growth Index (MGI) on Oriented Strand Board (OSB) and compared with alternative materials, Fiberboard, and Plywood. Water penetration rate, i.e. 1%, 2%, and 3% of wind-driven rain-deposited on a water-resistive barrier (WRB) with an air change rate (ACH) of 0 and 15 1/h in the drainage cavity was considered across all climatic zones (4, 6 and 7A) to accommodate the MGI below 3 following the ASHRAE 160-2021 standard 1% wind-driven rain. The location addressing the performance or mould growth is within 0.5 mm of the exterior side of the sheathing board.

# Chapter 2: Literature Review

Global temperatures increase the severity of climate-related events, including heat waves, droughts, wildfires, storms, and wind-driven rain[16] [17]. The fast-paced climate change poses significant challenges to construction durability, particularly affecting the moisture performance of wood-structured buildings. This necessitates adopting strategies to mitigate the effect of building enclosures exposed to wind-driven rain and wind loads, decreasing the risk of premature deterioration. The envelope exhibits increased susceptibility to environmental factors among building systems, as its hygrothermal characteristics determine how individual components withstand stress and undergo degradation over time.

Rainwater penetration through wall assemblies and compromised building envelope barriers accelerates building deterioration by promoting mould growth and decay. Hygrothermal modelling techniques ease the long-term rainwater risk evaluation of wall assemblies. Simulation tools like WUFI, hygIRC, DELPHIN and COMSOL Multiphysics offer 1D, 2D, and 3D analysis capabilities, requiring a comprehensive understanding of wall assembly responses to both direct and infiltrating moisture conditions and the selection of representative climate data. WUFI, hygIRC, and DELPHIN utilize gradients in moisture content, relative humidity, and capillary pressure as the driving forces for liquid water movement within porous materials. In contrast, the COMSOL module for heat and moisture transfer in porous building materials primarily uses the relative humidity gradient to facilitate moisture transfer [18].

Linden and Bossche identified several factors affecting the amount of water interacting with and penetrating the exterior cladding of building envelopes, including surface spreading, rebounding, adhesion and evaporation, droplet splashing and fragmentation, gravitational runoff, and penetration through the cladding material [19]. ASHRAE Standard 160 establishes "Criteria for Moisture-Control Design Analysis in Buildings"[9]; hygrothermal simulations should incorporate a default moisture load equivalent to 1% of the total rain impact on the cladding. The moisture load specified here is intended to be applied at the outer surface of the weather-resistive barrier (WRB). The penetration rate mentioned includes water movement before reaching the WRB, such as downward water flow behind the exterior cladding. If a WRB is absent, the placement for applying the moisture load must be determined through a technical analysis and justified accordingly. Due to limited data on penetration rates for different exterior cladding types, numerous studies have adopted a 1% wind-driven rain load as the benchmark for rainwater penetration, applying it to the weather-resistive barrier to assess its impact on the long-term performance of wall assemblies [19].

National Research Council Canada (NRC) has generated climate data to perform hygrothermal simulations for 564 locations. The availability of bias-corrected climate time series realizations from the CanRCM4-LE model for the baseline period (1986-2016) and future scenarios of 2°C and 3.5°C global warming temperature rise significantly facilitates the evaluation of hygrothermal performance under projected climate conditions. The generated data years include Typical Meteorological Year (TMY) for energy applications, Typical Downscaled Year (TDY), Extreme Cold Year (ECY) and Extreme Warm Year (EWY) and Moisture Reference Years (MRYs) for hygrothermal applications based on Moisture Index (MI) [4]. However, selecting moisture reference years can be accomplished through various methodologies, incorporating indices such as climate, moisture, and RHT [20]. According to ASHRAE Standard 160-2021, moisture performance evaluation of wall assemblies requires a Moisture-design Reference Year (MRY) selected based on the Severity Index, which is the year representing the 93rd percentile or the second highest of severity index values derived from a 30-year weather data analysis [9].

To examine the effectiveness and reliability of MRY selection methods, i.e., Severity Index ($I_{sev}$), Climatic Index (CI), and Moisture Index for long-term hygrothermal analysis, several studies have been conducted in recent years. A conclusive approach by Aggarwal et al. indicated that the $I_{sev}$ method better predicted worst-case moisture scenarios[21]. However, different wall assemblies require varying MRY repetitions to match 31-year simulation results, particularly noting distinctions between wet and dry cities[21], [22]. Hygrothermal simulations of brick veneer assembly under ASHRAE 1% wind-driven rain moisture revealed that $I_{sev}$ yielded higher mould indices of 4 on the oriented strand board (OSB) sheathing than the MI approach.

Additionally, north-facing $I_{sev}$ calculations proved more representative than directional wind-driven rain analysis for moisture behaviour prediction [23]. Another research employing Delphin 5.9 software revealed that north orientation led to the worst moisture performance of OSB in well-protected walls, while the orientation receiving the maximum annual WDR typically showed the poorest performance for moisture accumulation for the ASHRAE rain exposure limit and established the necessity of hourly WDR distribution analysis for accurate, critical orientation selection [24]. A similar conclusion was identified by Aggarwal et al., emphasizing the importance of considering orientation-specific design strategies in moisture management [25].

The "Guidelines on Design for Durability" report by M. Lacasse emphasizes that analyzing the hygrothermal performance of building components requires a comprehensive framework that includes performance attributes, criteria, and evaluation processes [26]. One of the critical performance criteria is the susceptibility of wooden materials to fungal growth[27] [26]. The sensitive class of material having a level of RH $\geq$ 80 favours mould growth as a function of surface temperature.[9]. This deterioration is a significant concern for indoor air quality (IAQ) and occupant health. The ASHRAE standard 160-2021 suggests the safe limit value remains $\leq$ 3 to avoid visible growth [9].

The MEWS (Moisture Management of Exterior Wall Systems) Project, Task 6, concluded that within a wall assembly, 75% of the water penetrated through the cladding, which accounts for 10-15%, drained in the air cavity. Based on these results, Defo et al. analyzed brick veneer walls under historical (1986-2016) and future (2062-2092) climate data, using a 0.3% moisture penetration rate. Based on RH and T calculated at the 0.5 mm OSB panel exterior layer via hygrothermal simulations, internal areas were resilient to mould, while coastal regions showed higher risks. Alternative designs improved performance, lowering the mould index from 3.6 to 3.9 in Vancouver and 2.0 to 1.65 in Halifax [28]. However, Olsson's laboratory tests summarized that under heavy WDR penetration rates (0.01-0.05 l/min) at the building façade, minor deficiencies could deposit a water penetration corresponding to 2% [29].

A DELPHIN software simulation study with a 1% moisture source on cross-laminated timber (CLT) wall under historical (1986-2016) and future (2062-2092) climates showed an increase in mould risk across five Canadian cities, with Ottawa experiencing the highest growth (1432%), followed by Calgary (149%) and Winnipeg (290%). Historically, Vancouver and St. John's already had high moisture risks [30]. A study on the effects of increased moisture sources on an Oriented Strand Board (OSB) within an External Thermal Insulation Composite System (ETICS) wall revealed that rain leakage levels of 1% and 2% do not cause moisture-related issues. However, 3% and 4% leakage results in a risky moisture content exceeding 20% in the OSB sheathing [31]. Wang and Ge's stochastic modelling approach with varying rain leakage positions and deposition rates (0.35%, 0.5% and 1%) revealed that rain penetration at the exterior surface of the oriented strand board (OSB) sheathing generated the highest moisture content and corresponding mould growth index (MGI) values. Interior surface rain deposition demonstrated significant mould proliferation potential in both east and south orientations for I-joist and exterior insulated assemblies [32].

Recent studies used the moisture index method to select MRYs from the generated climate data. However, ASHRAE 160-2021 proposed a Severity Index ($I_{sev}$) to select an MRY as severe weather to evaluate the moisture and mould growth performance. The present study analyzes the mould growth for historical climatic data (1986-2016) using $I_{sev}$ MRY method on an NBC 2020 code compliance brick veneer wall. The calculation period has been set at seven years, during which two wall orientations were analyzed: one that receives minimal solar radiation and the other that is subjected to the maximum wind-driven rainfall. Each orientation analyzed three rain penetration cases (1%, 2%, and 3% of wind-driven rain) and two Air Change Rates (ACH 0 and ACH 15) in the drainage cavity. The key aspect is noted on the outer surface of the sheathing board to assess the impact of the hygrothermal response, relative humidity (RH), and temperature (T) on mould development on the sheathing surface boards. The materials, including OSB, Fiberboard, and Plywood, were selected, and a point situated 0.5 mm from the outer surface was chosen to generate data on temperature and relative humidity, aiding in the determination of the Mold Index and the rate of mould growth as performance indicators.

# Chapter 3: Research Methodology

This chapter includes the methodology adopted to compute the mould growth results. The brick veneer wall investigated for mould performance is detailed in section 3.1. The weather data used to develop the Moisture Reference Year and variables to generate the climate file are detailed in sub-chapters 3.2 and 3.3. Section 3.4 outlines the method of MRY selection, i.e., the Severity Index. Moisture design criteria, Canadian cities and their diverse climatic features are discussed in Sections 3.5 and 3.6, respectively. The simulation software and mould growth model are discussed in Section 3.7, and boundary conditions are outlined in Section 3.8.

## 3.1 Wall configuration:

This study examines a wall assembly design adapted from the seminal research of M. Defo et al. to evaluate the moisture penetration and mould resistance for wall components in low-slope, multi-story wooden frame structures [3]. The wood frame wall with red matt clay brick veneer cladding meets the minimal requirement prescribed in Part 9 of NBCC [3]. The analysis encompasses a building with a low-slope roof and a multi-story wooden frame structure ranging from 10 to 15 meters in height, with particular attention to the performance of different sheathing materials under varying water ingress to assembly.

Wall Assembly Configuration: Figure – 2 shows the baseline wall assembly comprises multiple layers, strategically arranged from the exterior (Left) to the interior (right) as follows:

- Exterior Cladding: Red matt clay brick
- Ventilation: Drainage cavity for moisture management
- Weather Protection: Sheathing membrane
- Structural Component: Sheathing board
- Thermal Insulation: Mineral fibre
- Vapor Control: Polyethylene vapor barrier
- Interior Finish: Gypsum board finished with latex primer and paint

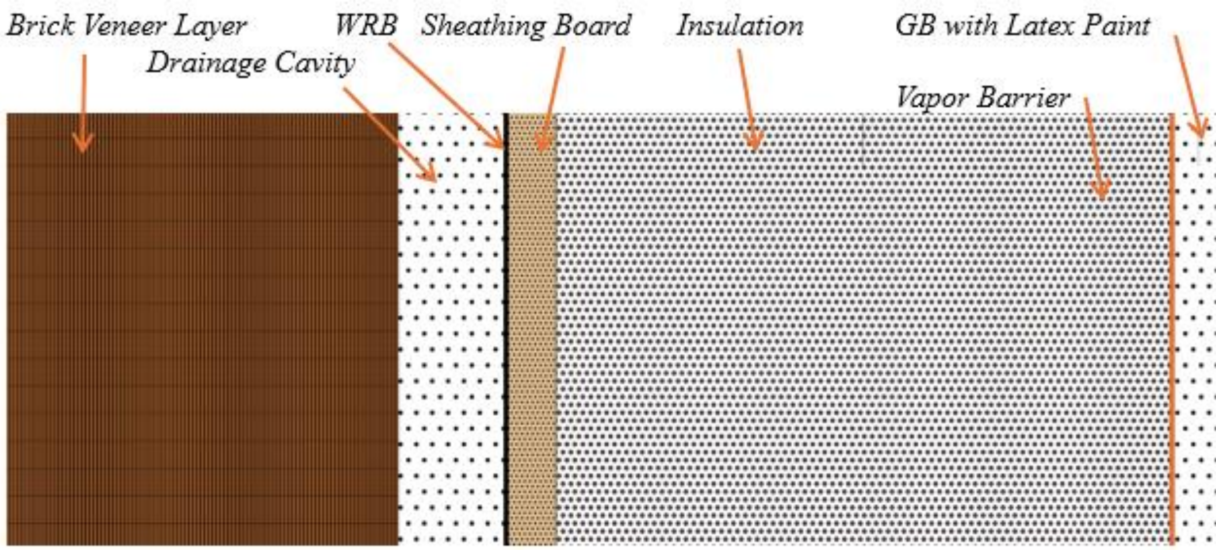


*Figure 2: Brick Veneer Wall Configuration (WUFI Simulation)*

The National Building Code of Canada (NBCC) stipulates a minimum 25-mm drained and vented air space that functions as a capillary break. [3], for all wood-frame walls with brick veneer cladding across Canadian jurisdictions

The investigation explores alternative designs by substituting the standard sheathing board with three different materials:

- Oriented Strand Board (OSB)
- Fiber Board (FB)
- Plywood

The study evaluates these configurations under controlled conditions where the sheathing membrane is exposed to wind-driven rain (WDR) penetration ranging from 1% to 3%. Given that the sheathing board represents a critical component vulnerable to moisture-related deterioration, particular emphasis is placed on analyzing mould growth potential on its exterior surface.

*Table 1: Wall components and their properties as per the NRC materials database [33]*

| Layer | Dimension of layer [3] (mm) | Dry Density kg/m3 | Specific Heat Capacity (J/kg. K) | Thermal Conductivity (W/m. K) | Porosity (m3/m3) |
|---|---|---|---|---|---|
| **Red Clay Brick** | 90 | 1900 | 800 | 0.500 | 0.213 |
| **Drainage cavity** | 25 | 1.2 | 1214 | 0.151 | - |
| **Sheathing membrane** | 0.22 | 909 | 1256 | 0.159 | 0.973 |
| **OSB** | 11 | 600 | 1800 | 0.094 | 0.960 |
| **Fibreboard** | 10.5 | 264.5 | 1880 | 0.049 | 0.950 |
| **Plywood** | 12 | 578 | 1880 | 0.098 | 0.960 |
| **Mineral fiber Insulation** | 140 | 11.5 | 840 | 0.043 | 0.999 |
| **Vapour barrier** | 0.15 | 1256 | 840 | 0.159 | 0.251 |
| **Gypsum Board** | 12.7 | 700 | 870 | 0.160 | 0.400 |

The analyzed wall assembly was designed as a new, unconditioned structure with initial moisture content constant across the assembly at 80% relative humidity. While wall construction, material properties, and moisture sources, including condensation from air and rain, can significantly influence performance outcomes, this study specifically focused on cases involving rain leakage and sheathing board performance. Material properties for wall components were established as per the research by Defo et al. research [8], utilizing data from the National Research Council Canada's (NRC) hygrothermal material property database (See Table 1) [33].

## 3.2 Weather File Generation

Building upon the framework established by Gaur et al. [34], who developed comprehensive standardized weather datasets for hygrothermal building simulations; this study accessed their publicly available time series data through their online platform [35]. This hygrothermal analysis encompassed a 31-year historical period (1986-2016). Following the methodological framework adopted by Aggarwal and Defo, the median realization was selected from a set of 15 climate realizations/runs ranked by the Moisture Index (MI) [24]. The selected run was then used to rank 31 years based on the ASHRAE Severity Index (section 3.4). The decided year is the Moisture Design Reference Year, representing the worst year, to conduct hygrothermal simulations for the selected cities, focusing on mould growth index performance. In the climate data generated by Gaur et al., the necessary climate variables listed in Table 2 were identified for undertaking hygrothermal and whole-building simulations [34].

*Table 2: Climate variables for weather file generation*

| S. No. | Climate variables | Units |
|---|---|---|
| **1** | Direct horizontal irradiance | $kJ/m^2$ |
| **2** | Diffused horizontal irradiance | $kJ/m^2$ |
| **3** | Direct normal irradiance | $kJ/m^2$ |
| **4** | Global horizontal irradiance | $kJ/m^2$ |
| **5** | Total Cloud Cover | % |
| **6** | Rainfall | mm |
| **7** | Wind Direction | Degree clockwise from north |
| **8** | Wind Speed | m/s |
| **9** | Relative Humidity | % |
| **10** | Temperature | °C |
| **11** | Atmospheric Pressure | Pa |
| **12** | Snow Cover | 0 (no snow) or 1 (snow) |

## 3.3 Moisture Design Reference Year

A Moisture Design Reference Year (MRY) is a critical concept in building science representing a selected year of weather data used for hygrothermal building envelope simulations. It captures moisture-related stresses that building envelopes may experience, including temperature, relative humidity, precipitation, and wind-driven rain. ASHRAE recommends selecting the MRY based on the Severity Index, explicitly using the 93rd percentile or the year with the second-highest severity index in thirty years[9]. The $I_{sev}$ approach was applied to the median weather data realization selected by Aggarwal and Defo [24]The severity index was calculated for each year within the median run, and the year with the second-highest severity index was chosen to prepare the climate file (.wac format) for WUFI Pro software. The WUFI climate variables are listed in Table 4. Based on the climate database, the north direction received the least solar radiation for all Canadian cities, given Canada's location in the Northern Hemisphere. The direction receiving the maximum wind-driven rain (WDR) is detailed in Table 3. Figure 3 shows the rain pattern and the direction receiving the maximum wind-driven rain.

*Table 3: Moisture Reference Year and Simulated Orientations*

| City | Median run | MRY ($I_{sev}$) | Least Solar Radiation Direction | WDR direction | Moisture source* (%) |
|---|---|---|---|---|---|
| **Calgary** | 10 | 2013 (15662) | North | North-West | 1 - 3 |
| **Ottawa** | 10 | 2009 (18504) | North | South-West | 1 - 3 |
| **Saskatoon** | 11 | 2012 (27456) | North | North-West | 1 - 3 |
| **Vancouver** | 4 | 2016 (18698) | North | South-East | 1 - 3 |

**Fraction of Rain Load*

*Table 4: WUFI Climate File Variables*

| S. No. | Climate variables | Units |
|---|---|---|
| **1** | Air Temperature | °C |
| **2** | Relative Humidity | % |
| **3** | Diffused solar radiation | $W/m^2$ |
| **4** | Global solar radiation | $W/m^2$ |
| **5** | Cloud Index | 0 - 1 |
| **6** | Rain | $L/m^2.h$ |
| **7** | Wind Direction | Degree clockwise from north |
| **8** | Wind Speed | m/s |
| **9** | Atmospheric Pressure | hPa |

# 3.4 Severity Index

The Severity Index ($I_{sev}$) is formulated from predicted values of RHT ($RHT_{predicted}$), which are determined using a regression function of the average annual value of multiple environmental parameters such as ambient air temperature, relative humidity, solar radiation on the wall surface, cloud cover, WDR on the wall, vapour pressure, wind speed, wind direction and coefficients.[36]. Based on ASHRAE 160-2021, the severity index ($I_{sev}$) for each year is calculated according to Equation (1):

$$I_{sev} = 108307 - 241 * Ev - 1391 * I_{cl} - 312326 * \phi + 183308 * r_{wd} + 15.2 * p_v + 27.3 * T_o^2 + 261079 * \phi^2 - 0.00972 * p_v^2$$ ……………………………*Equation 1: Severity Index Calculation*

Where:

- Ev is the solar radiation (W/m²) incident on the wall receiving the least radiation

- $I_{cl}$ is the cloud index (ranging from 0 – 8)
- $\phi$ is the relative humidity, 0 – 1
- $r_{wd}$ is the wind-driven rain ($kg/m^2 \cdot h$) on the wall
- $p_v$ is vapour pressure (Pa)
- $T_o$ is the ambient temperature (°C)

Following the prescribed methodology, the severity index ($I_{sev}$) was calculated for the north-facing orientation, which receives the minimum solar radiation. All weather parameters were computed as annual average values, utilizing hourly data throughout each year of the analysis period.

## 3.5 Moisture Design Criteria

In hygrothermal simulation models, determining accurate moisture penetration rates through different building materials and wall systems remains challenging due to limited empirical data [32].ASHRAE established Committee 160P in 1996 to investigate how moisture affects building deterioration and to develop preventive guidelines [5]. . The deposit site for this moisture is modelled as reaching the weather-resistive barrier's (WRB) outer face when conducting building envelope simulations. The ASHRAE Standard 160, updated in 2021, is the primary reference for this project's exterior wall assembly design, specifically adapted for Canadian climatic conditions. A key modification in this revision concerns the Moisture Design Reference Year (MDRY/MRY) methodology. The new standard defines MRY using the 93rd percentile year or the second highest year of the severity index for hygrothermal performance, analyzed over a 30-year weather data period. This represents a significant shift from the previous approach, which relied on the 10th percentile cold and warm year calculations [37]. For moisture control design analysis, the standard outlines two acceptable approaches for weather data implementation:

- Using the Moisture Design Reference Year
- Analyze using10 consecutive years of hourly meteorological data

The guidelines mandate performance evaluation of wall assemblies in at least two distinct orientations:

- The direction receiving minimal annual solar radiation

- The orientation experiencing maximum wind-driven rain exposure, calculated using specified mathematical formulations

$r_{wd} = C * U * r_h^{0.88} * cos\,\Theta$ ……………………..…. *Equation 2: ASHRAE 160 Wind-Driven Rain*

Where, $r_{wd}$ = wind-driven rain, kg/m$^2$.h

C = Empirical constant, 0.222

U = hourly average wind speed at 10m above ground level, m/s

$r_h$ = rainfall intensity on a horizontal surface, mm/h

ϴ = angle between wind direction and normal to the wall

As per ASHRAE 160, a minimum analysis of five consecutive $I_{sev}$ MRY evaluates moisture accumulation simulation to minimize mould growth, ensuring the maximum total moisture content of assembly at the end of the final year does not exceed that of the previous year.

To meet the performance criteria, the Mold Growth Index (MGI) should not exceed a value of three [9]. An MGI of three indicates visible mould findings by the human eye on the surface, with less than 10% coverage or, under a microscope, less than 50%. These model criteria were given in the research conducted by Ojanen et al. [38].

# 3.6 Selected Cities

This study focuses on four distinct cities, each depicted in Table 5. The selected cities exhibit diverse climatic features. The Moisture Indices (MIs) for Vancouver, Calgary, Ottawa, and Saskatoon are 1.93, 0.37, 0.84, and 0.41, respectively. [24]. Figure 4 shows the difference and the range for the temperature, Rainfall and wind speed for all four cities.

*Table 5: Selected cities for Hygrothermal analysis*

| City | Median run[24] | Moisture index | Climate Zone | Latitude (º) | Longitude (º) | Time Zone | Rainfall mm |
|---|---|---|---|---|---|---|---|
| **Calgary** | 10 | 0.37 | 7A | 51.1 | -114.1 | -7 | 360 |
| **Ottawa** | 10 | 0.84 | 6 | 45.3 | -75.4 | -5 | 760 |
| **Saskatoon** | 11 | 0.41 | 7A | 52.17 | -106.70 | -6 | 310 |
| **Vancouver** | 4 | 1.93 | 4 | 49.3 | -123.1 | -8 | 1250 |

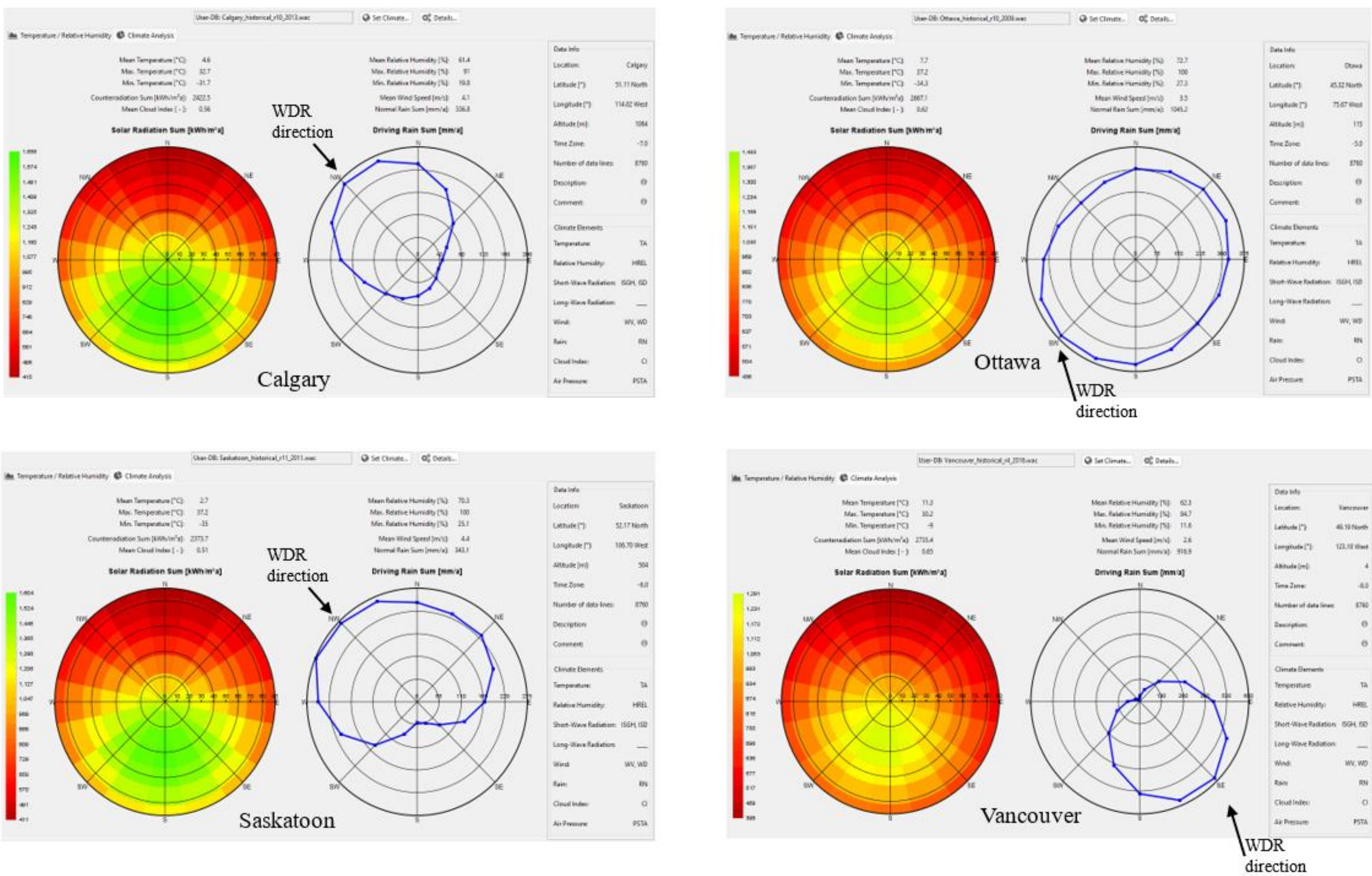


*Figure 3: Solar radiation and Wind-driven rain patterns for the selected cities based on MRY – WUFI simulation screen*

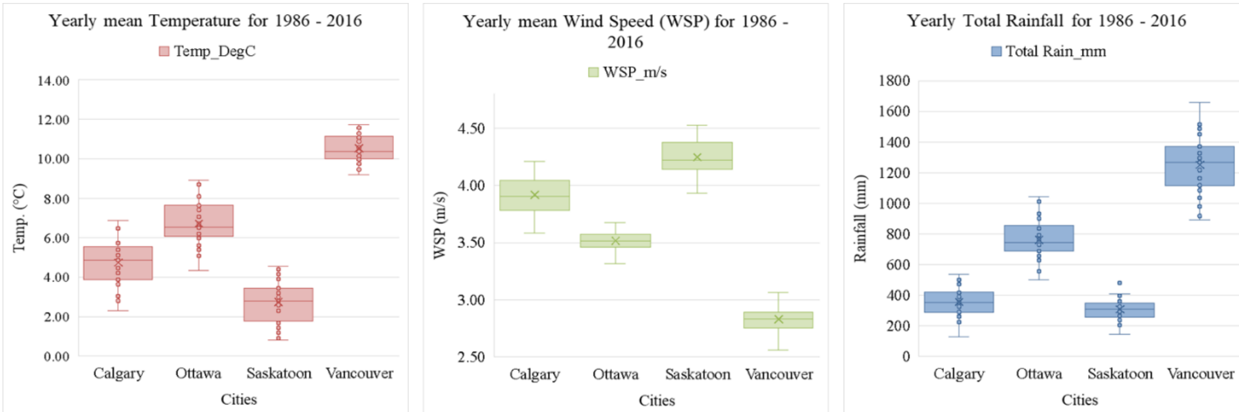


*Figure 4: Temperature, Rainfall and Wind Speed variables for the Selected Cities*

# 3.7 Numerical Models

## 3.7.1 Hygrothermal simulations – WUFI® Pro 6.8

WUFI (Wärme Und Feuchte Instationär), which translates from German to "Transient Heat and Moisture transport" [39], serves as the primary simulation tool in this study. This advanced hygrothermal modelling software enables the dynamic analysis of coupled heat and moisture transport through building envelope components under realistic climate conditions. WUFI® Pro is the standard program for performing one-dimensional hygrothermal analysis of building envelopes under real climate conditions considering built-in moisture, driving rain, solar radiation, long-wave radiation, capillary transport, and summer condensation [40]. Incorporating the WUFI® Pro 6.8 Non-commercial version, the hygrothermal performance simulations were conducted under initial conditions of 80% relative humidity and a component temperature of 20°C. The interior building temperature was maintained at 21.1°C in compliance with ASHRAE Standard 160. The simulations were executed over seven years, from January 1, 2020, to December 31, 2027, to ensure steady-state conditions and optimal results. The seven years was selected to compute the long-term mould growth considering the cyclic behaviour of mould growth due to the variation in Relative Humidity (RH) and Temperature (See Appendix 2 – Figure 19-21)

## 3.7.2 Mould Growth Calculation

Mold growth within building materials is a significant concern, particularly when the relative humidity exceeds 60% [41]. ASHRAE Standard 160-2021 defines the Relative Humidity (RH) of 80% as the threshold criterion for mould growth risk assessment at material surfaces[9].

Software like WUFI Pro cannot assess condensation and mould growth risk individually. [42]. Assessing mould growth potential requires sophisticated analytical tools that extend beyond basic hygrothermal simulations. WUFI® Pro, a leading hygrothermal simulation software, incorporates two specialized post-processing tools: WUFI® Bio (bio-hygrothermal model) and WUFI® VTT (updated VTT/Viitanen model) [43]. These tools enable simultaneous evaluation of mould growth indices and rates while performing comprehensive hygrothermal analysis of building assemblies.

The Technical Research Centre of Finland (VTT) developed an empirical model, named the VTT/Viitanen model, that employs a six-step assessment of mould growth indices (Table 6) to quantify the mould growth in terms of Mould Index [44]. Through research by Hukka and Viitanen, the mathematical modelling of mould development under variable moisture conditions was advanced, and mould growth intensity on material surfaces was expressed as percentage coverage, [45] Their work resulted in the formulation of a novel equation (Equation 3) that specifically addressed the fungal growth dynamics of wood under fluctuating humidity environments.

$$\frac{dM}{dt} = \frac{1}{7.\exp\left(-0.68 lnT - 13.9 lnRH + 0.14W - 0.33SQ + 66.02\right)}\ k_1 k_2$$

*……………………………………………………… Equation 3: Mould growth model equation for wood*

Where T refers to the Temperature in degrees centigrade, RH is the Relative Humidity (%), W is the wood species (0 = pine and 1 = spruce), SQ is the surface quality ($SQ = 0$ for sawn surface, $SQ = 1$ for kiln-dried quality), and the coefficient $k_1$ indicates the intensity of mould growth, varying with the growth level, while $k_2$ moderates this intensity as the mould index $M$ nears its maximum. These coefficients adjust the fundamental mould model equation for different building materials.

*Table 6: Mould Growth Index for Modeling*

| Index | Description of growth rate |
|---|---|
| 0 | No growth |
| 1 | Small amounts of mould on the surface (microscope), initial stages of local growth |
| 2 | Several local mould growth colonies on the surface (microscope) |
| 3 | Visual findings of mould on the surface, < 10 % coverage, or < 50 % coverage of mould (microscope) |

| | |
|---|---|
| 4 | Visual findings of mould on the surface, 10 - 50 % coverage, or >50 % coverage of mould (microscope) |
| 5 | Plenty of growth on the surface, with> 50 % coverage (visual) |
| 6 | Heavy and tight growth, coverage about 100 % |

Building materials are categorized into distinct sensitivity classes based on their susceptibility to mould growth. ASHRAE 160 utilizes these classifications in its guidelines. The present research examines materials according to the mould sensitivity classifications recommended by ASHRAE standard 160.

*Table 7: Mould Sensitivity Classes for Various Materials*

| **Sensitivity Class** | **Defined By Ojanen et al. [38]** | **ASHRAE 160-2021[9] [38]** |
|---|---|---|
| Very Sensitive | Pine sapwood | Untreated wood includes lots of nutrients for biological growth |
| Sensitive | Glued wooden boards, PUR with paper surface, spruce | Planed wood, paper-coated products, wood-based boards |
| Medium Resistant | Concrete, aerated and cellular concrete, glass wool, polyester wool | Cement or plastic-based materials, mineral fibres |
| Resistant | Polyurethane with polished surface | Glass and metal products, materials with efficient protective compound treatments |

# 3.8 Boundary Conditions and Simulation Reliability

## 3.8.1 Simulation Quality

The simulation's numerical quality depends upon the two parameters, convergence failures or moisture balance, which were analyzed at the end of each simulation data (Figure 6). A high number of convergence failures indicates computational challenges in solving the governing equations, typically associated with elevated moisture content levels or significant moisture transport phenomena.[41]. While ideally, convergence failures should approach zero, the studied simulations' failure was considered within a range of 0-100 to cope with the high moisture ingress during simulation. Although modifying the component assembly design could potentially reduce convergence failures, this study maintained consistent wall configurations across different cities for comparative analysis.

Consequently, the focus shifted to optimizing the moisture balance (Figure 5) factor by minimizing the difference between the Moisture Balance (Balance 1 ~ Balance 2) value ($kg/m^2$) i.e., The change in 'total water content' during the calculation and the sum of the 'surface flows' [40] generated at the end of the simulation.

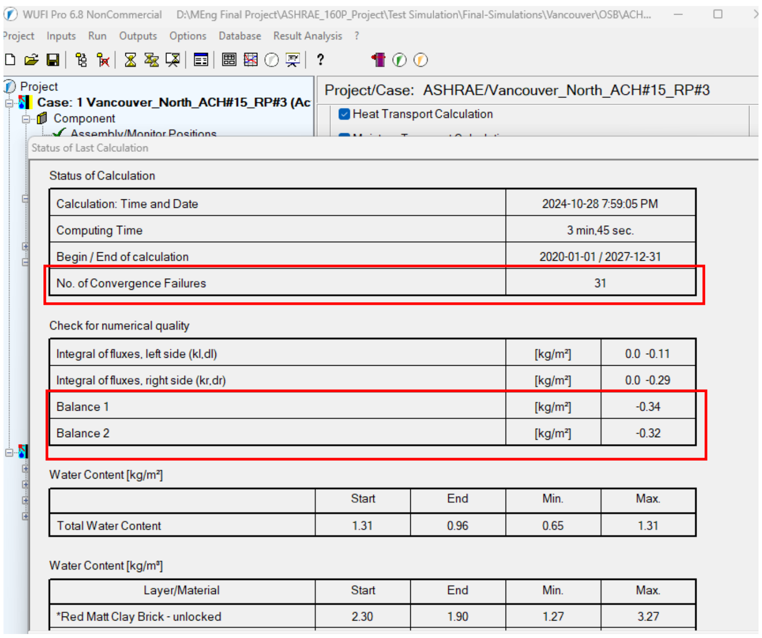


*Figure 5: Calculation Status dialog box - Convergence Failure and Moisture Balance*

This optimization was achieved by carefully controlling temporal discretization parameters: implementing Time step(s) = 1 hour and adaptive time step control with Number of Steps = 03 and Maximum number of Stages = 10, along with appropriate grid size adjustments. The number of steps determines the sub-steps into which the original Time step is subdivided. The maximum number of allowed stages determines how often WUFI can sub-sub-divide a step before it registers a convergence failure and proceeds with the next step (Figure 6) [40].

The software does not allow manual specification of grid numbers for individual layers [18]. In this analysis, predefined mesh densities of fine size in the range of 100 – 180 were used for the entire assembly. Subsequently, WUFI automatically determines the grid distribution and sizing across individual layers based on these parameters.

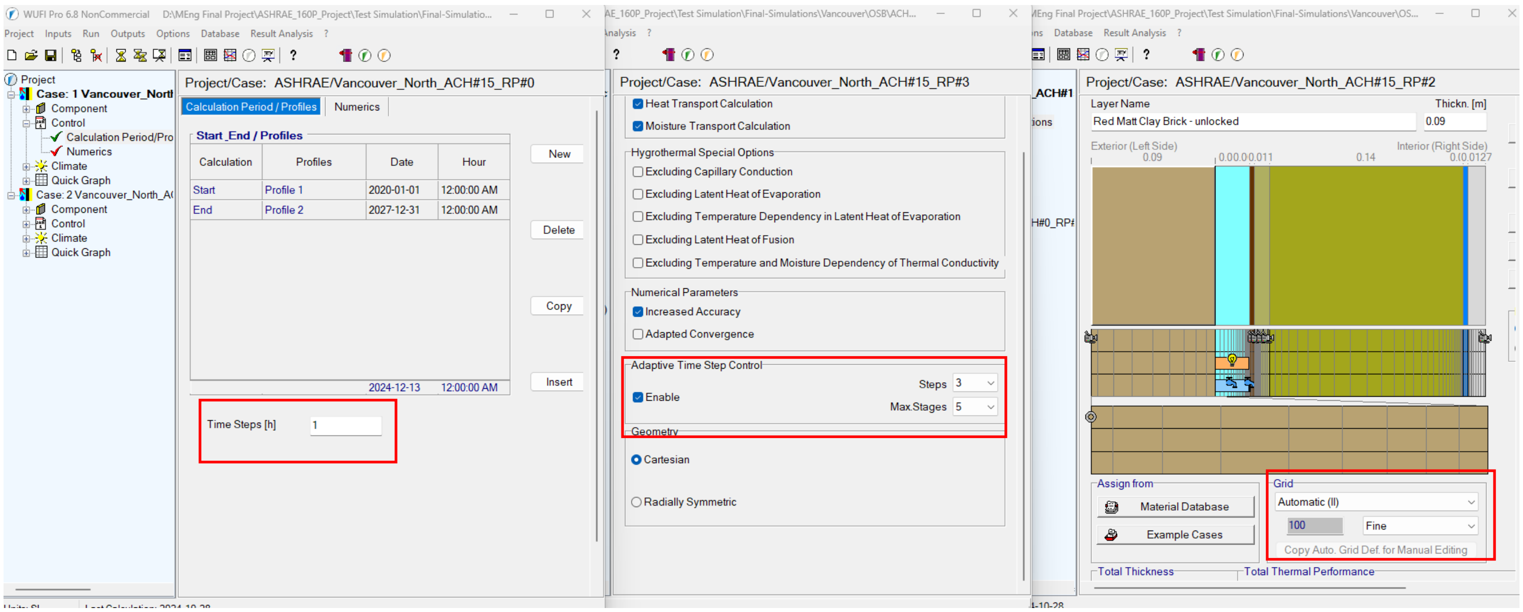


*Figure 6: Numeric control parameters to optimize the convergence failure and Moisture Balance Value*

### 3.8.2 Indoor and Initial Conditions

The initial conditions were 80% relative humidity and a component temperature of 20°C. Indoor conditions were standardized across all locations, with the temperature maintained at 21.1°C, with particular emphasis on heating and air conditioning systems, including dehumidification. To ensure consistent environmental parameters for the hygrothermal analysis across the four cities, indoor moisture levels were controlled at a relative humidity (RH) set point of 50%. The construction unit was assumed to be airtight, and in compliance with ASHRAE Standard 160, the moisture generation rate for a four-bedroom dwelling was set at $1.3 * 10^{-4}$ kg/s.

### 3.8.3 Outdoor Conditions

Based on each city's weather data, the analysis was conducted in two distinct orientations specified by ASHRAE Standard 160: one in the direction of minimal solar radiation and the other in the direction receiving the maximum wind-driven rain. The methodology for determining the direction of wind-driven rain (WDR) is detailed in the earlier sections.

Outdoor boundary conditions used to define various parameters are presented in Table 8. WUFI defines the rain load (adhering rain) as the amount of rainwater that touches the exterior surface of the cladding, which can be calculated as shown in equation 4 and the performed analysis was done with an adhering rain factor value of 0.7 (70%) for an exterior wall surface [46]. The additional rain load calculation can be calculated using the ASHRAE 160 rain load Equation 4.

$r_{bv} = F_E \cdot F_D \cdot F_L \cdot U \cdot cos(\Theta) \cdot r_h,$ ………………………………………………… *Equation 4*

- $r_{bv}$ Rain deposition on vertical wall (kg/m²h)
- $F_E$: Rain exposure factor
- $F_D$: Rain deposition factor
- $F_L$: empirical constant, 0.2 kgs/ (m³ mm)
- U: hourly average wind speed at 10 m height (m/s)
- ϴ: angle between wind direction and normal to the wall (°)
- $r_h$: rainfall intensity on a horizontal surface (mm/h)

The WUFI's rain load calculation, equation 5, is based on ASHRAE 160 Rain Load equation 4.

Rain Load=Rain * $F_E$ * $F_D$ * 0.2 s/m * Wind Velocity ……………………………… *Equation 5*

*Table 8: Boundary Conditions for Wall Assembly*

| **Initial Conditions** | |
|---|---|
| Temperature (°c) | 20 |
| Relative humidity (%) | 80 |
| **Rain load calculation** | |
| Rain exposure factor | 1.4 |
| Rain deposition factor | 0.5 |
| **Indoor conditions** | |
| Temperature (°c) | 21.1 |
| Relative humidity (%) | 50% |
| Moisture generation rate (kg/s) | $1.3 * 10^{-4}$ |
| **Outdoor conditions** | |
| **Exterior surface (left side)** | Value |
| Heat resistance ($m^2K/W$) | 0.588 |
| Long wave radiation ($w/m^2K$) | 6.5 |
| Short wave radiation absorptivity | 0.6 |
| Long wave radiation emissivity | 0.9 |
| Ground short wave reflectivity | 0.2 |
| Adhering a fraction of the rain | 0.7 |
| **Interior surface (right side)** | |
| Heat Resistance ($m^2K/W$) | 0.125 |
| sd value (m) (latex paint) | 0.7 |

# Chapter 4: Result and Analysis

This study investigates the mould growth potential of three different sheathing boards (OSB, Fiberboard, Plywood) using the hydrothermal tool WUFI® Pro and VTT model. The brick veneer wall's performance was evaluated based on the second-highest severity year between 1986-2016 for different climate zones. The criteria for distinction were based on rainwater penetration and air changes per hour (ACH) for the two wall orientations: (i) the least solar radiation and (ii) the wall facing the maximum wind-driven rain direction. The calculation period of seven years aligns with the fact that MGI does not reach its maximum value in a year; instead, it follows a cyclic curve of high and low MGI values if ventilation is considered (Appendix 2 – Figure 18-20). Table 9 details the maximum mould growth index, and the number of years, it reaches its max value over the simulation period of seven years.

Figure 7 illustrates the predicted risk of mould growth on the outer layer of various types of sheathing boards in Vancouver under severe weather year selected based on a 31-year weather dataset (1986-2016) using the severity index ($I_{sev}$) method. The effect of the 1% on OSB evaluated by Shayoun et al. for the $I_{sev}$ method aligned with the results for the Vancouver climate zone for a historical period with MGI = 0 [23]. However, the rain load calculation approach was adopted differently.

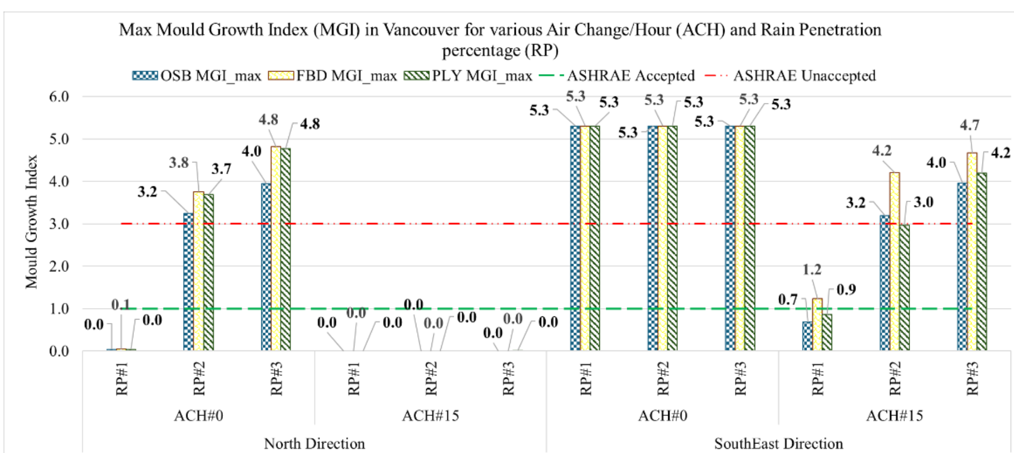


*Figure 7: Maximum Mould Growth Index for Vancouver City*

The trend for the Mould Growth Index (MGI) on sheathing materials facing severe rain, particularly to the southeast, showed consistent results, with an MGI of 5.3 even with just 1% rain accumulation, not considering ventilation within the drainage cavity. However, with an ACH of 15 and a 1% moisture source, the potential for wood mould growth was reduced by 40%, remaining within the concerned limits 1<MGI<3. The 12 ACH was not sufficient to mitigate the MGI >5 for brick wall [23]. In contrast, 15 ACH was inadequate to address the issue of higher water penetration (i.e., >1% WDR) in the third layer of defence, the sheathing board. The wall performed best when oriented in the direction with the least solar radiation, typically the north. Ventilation in the drainage cavity effectively facilitated the drying of the wall, maintaining an MGI of 0.

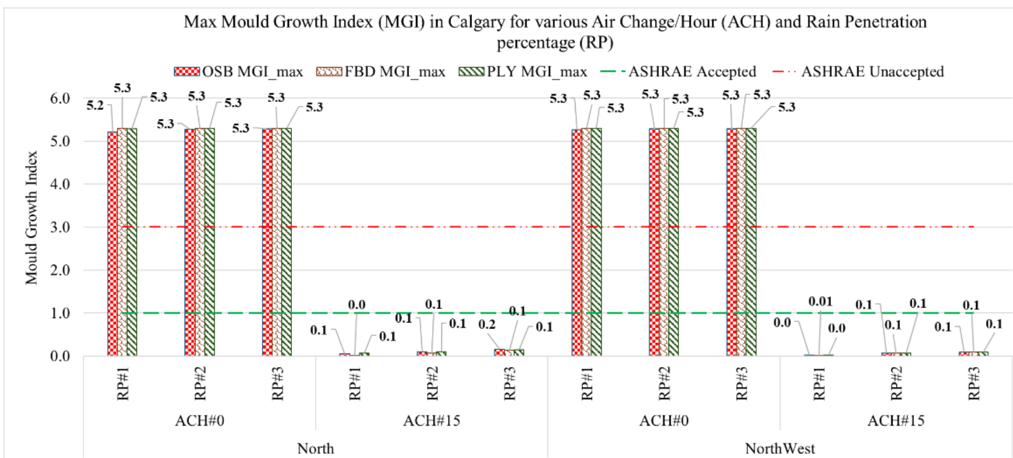


*Figure 8: Maximum Mould Growth Index for Calgary city*

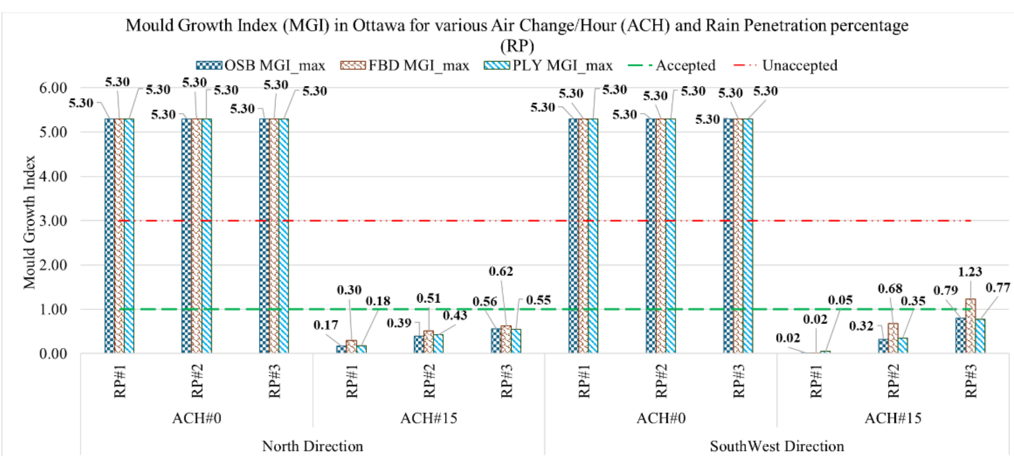


*Figure 9: Maximum Mould Growth Index for Ottawa city*

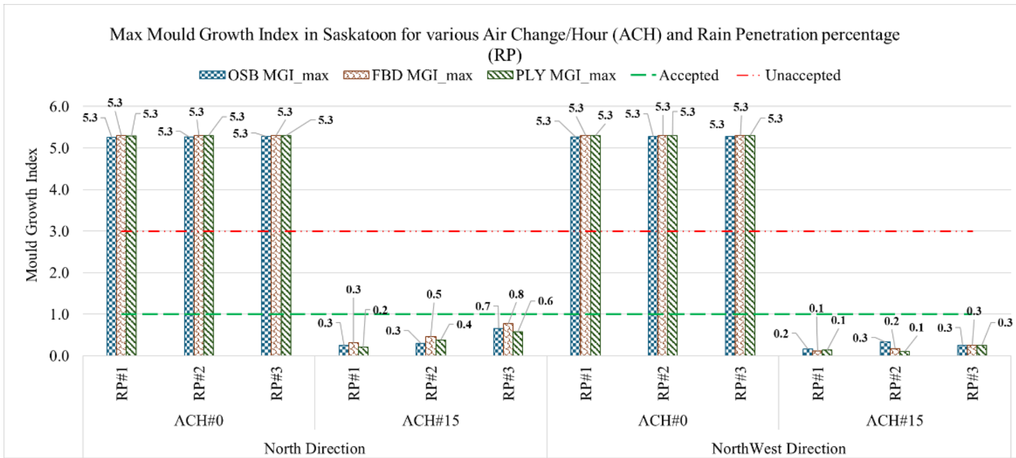


*Figure 2: Maximum Mould Growth Index for Saskatoon city*

Figures 8, 9 and 10 show that when evaluating the performance of this wall in Canadian Climate Zones 6 and 7A, the worst outcomes were observed for the non-ventilated north-oriented wall. In Ottawa, a maximum mould growth index value of 5.3 was recorded, even considering the lowest rain load on the water-resistive barrier. Similarly, in Saskatoon and Calgary, OSB, fiberboard, and plywood materials experienced a significantly higher level of mould growth. The hygrothermal simulation results conducted for Vancouver indicate a significantly lower susceptibility to mould growth in the third layer of defence for both orientations recommended by the ASHRAE 160 standard, provided that an air change rate (ACH) of 15 is consistently maintained. Additionally, for rain penetration rates of 1%, 2%, and 3%, the Mould Growth Index (MGI) recorded for Calgary was consistently 0.1 across all three materials. A similar performance was observed in Saskatoon; however, an exception was noted in the northwest orientation, where the MGI was half that of the north orientation, maintaining the MGI value below 0.6.

In the Ottawa region, the influence of wind-driven rain direction has raised concerns regarding wall configuration for mould growth assessment, particularly compared to the standard direction. For Fiberboard in the southwest orientation with a ventilation rate of 15 ACH, the MGI was evaluated at 1.2 for a 3% wind-driven rain case

*Table 9: Maximum Mould Growth Index (MGI) and Years to reach max MGI for the selected sheathing materials.*

| Location | Direction | Air Change per Hour | % Rain Deposit | OSB | | Fiberboard | | Plywood | |
|---|---|---|---|---|---|---|---|---|---|
| | | | | MGI (max) | Years to MGI (max) | MGI (max) | Years to MGI (max) | MGI (max) | Years to MGI (max) |
| **Vancouver** | North | ACH#0 | RP#1 | 0.0 | 0.0 | 0.1 | 7.4 | 0.0 | 7.0 |
| | | | RP#2 | 3.2 | 7.7 | 3.8 | 7.7 | 3.7 | 7.7 |
| | | | RP#3 | 4.0 | 8.0 | 4.8 | 7.7 | 4.8 | 7.7 |
| | | ACH#15 | RP#1 | 0.0 | 0.0 | 0.0 | 0.0 | 0.0 | 0.0 |
| | | | RP#2 | 0.0 | 0.0 | 0.0 | 0.0 | 0.0 | 0.0 |
| | | | RP#3 | 0.0 | 0.0 | 0.0 | 0.0 | 0.0 | 0.0 |
| | Wind Driven Rain | ACH#0 | RP#1 | 5.3 | 3.6 | 5.3 | 1.6 | 5.3 | 1.6 |
| | | | RP#2 | 5.3 | 2.6 | 5.3 | 1.5 | 5.3 | 1.6 |
| | | | RP#3 | 5.3 | 2.6 | 5.3 | 1.4 | 5.3 | 1.6 |
| | | ACH#15 | RP#1 | 0.7 | 6.1 | 1.2 | 3.1 | 0.9 | 7.0 |
| | | | RP#2 | 3.2 | 7.2 | 4.2 | 7.1 | 3.0 | 7.2 |
| | | | RP#3 | 4.0 | 7.3 | 4.7 | 7.0 | 4.2 | 7.2 |
| **Ottawa** | North | ACH#0 | RP#1 | 5.3 | 2.6 | 5.3 | 2.6 | 5.3 | 4.8 |
| | | | RP#2 | 5.3 | 1.7 | 5.3 | 2.5 | 5.3 | 2.8 |
| | | | RP#3 | 5.3 | 4.6 | 5.3 | 6.6 | 5.3 | 0.8 |
| | | ACH#15 | RP#1 | 0.1 | 5.5 | 0.3 | 7.5 | 0.1 | 4.8 |
| | | | RP#2 | 0.3 | 2.5 | 0.5 | 3.6 | 0.4 | 2.8 |
| | | | RP#3 | 0.5 | 2.5 | 0.6 | 4.5 | 0.5 | 2.8 |
| | Wind Driven Rain | ACH#0 | RP#1 | 5.3 | 1.8 | 5.3 | 2.6 | 5.3 | 6.3 |
| | | | RP#2 | 5.3 | 0.5 | 5.3 | 2.4 | 5.3 | 3.8 |
| | | | RP#3 | 5.3 | 4.8 | 5.3 | 4.6 | 5.3 | 7.3 |
| | | ACH#15 | RP#1 | 0.0 | 0.0 | 0.0 | 0.0 | 0.0 | 0.0 |
| | | | RP#2 | 0.3 | 2.8 | 0.6 | 2.6 | 0.3 | 1.3 |
| | | | RP#3 | 0.7 | 0.5 | 1.2 | 2.5 | 0.7 | 6.8 |
| **Calgary** | North | ACH#0 | RP#1 | 5.2 | 4.7 | 5.3 | 7.7 | 5.3 | 0.4 |
| | | | RP#2 | 5.3 | 3.7 | 5.3 | 5.7 | 5.3 | 0.8 |
| | | | RP#3 | 5.3 | 7.6 | 5.3 | 7.6 | 5.3 | 0.4 |
| | | ACH#15 | RP#1 | 0.1 | 7.6 | 0.0 | 7.6 | 0.1 | 0.8 |
| | | | RP#2 | 0.1 | 7.7 | 0.1 | 7.6 | 0.1 | 0.4 |
| | | | RP#3 | 0.2 | 6.7 | 0.1 | 7.6 | 0.1 | 0.8 |
| | Wind Driven Rain | ACH#0 | RP#1 | 5.3 | 0.4 | 5.3 | 5.7 | 5.3 | 0.4 |
| | | | RP#2 | 5.3 | 0.8 | 5.3 | 4.7 | 5.3 | 5.8 |
| | | | RP#3 | 5.3 | 0.4 | 5.3 | 7.6 | 5.3 | 0.4 |
| | | ACH#15 | RP#1 | 0.0 | 0.0 | 0.0 | 0.0 | 0.0 | 0.0 |
| | | | RP#2 | 0.1 | 0.4 | 0.1 | 7.6 | 0.1 | 0.4 |
| | | | RP#3 | 0.1 | 1.8 | 0.1 | 7.7 | 0.1 | 0.4 |
| **Saskatoon** | North | ACH#0 | RP#1 | 5.3 | 7.6 | 5.3 | 5.7 | 5.3 | 7.6 |
| | | | RP#2 | 5.3 | 7.6 | 5.3 | 4.8 | 5.3 | 7.6 |
| | | | RP#3 | 5.3 | 7.6 | 5.3 | 4.7 | 5.3 | 7.7 |
| | | ACH#15 | RP#1 | 0.3 | 0.6 | 0.3 | 0.6 | 0.2 | 0.5 |
| | | | RP#2 | 0.3 | 0.6 | 0.5 | 0.6 | 0.4 | 0.6 |
| | | | RP#3 | 0.7 | 0.6 | 0.8 | 1.6 | 0.6 | 0.6 |
| | Wind Driven Rain | ACH#0 | RP#1 | 5.3 | 7.6 | 5.3 | 4.7 | 5.3 | 7.6 |
| | | | RP#2 | 5.3 | 7.6 | 5.3 | 4.7 | 5.3 | 7.6 |
| | | | RP#3 | 5.3 | 7.6 | 5.3 | 3.7 | 5.3 | 7.7 |
| | | ACH#15 | RP#1 | 0.2 | 0.3 | 0.1 | 0.3 | 0.1 | 0.3 |
| | | | RP#2 | 0.3 | 0.5 | 0.2 | 0.3 | 0.1 | 0.3 |
| | | | RP#3 | 0.3 | 0.6 | 0.3 | 0.6 | 0.3 | 0.6 |

The data was observed and analyzed based on the percentage of time the Mold Growth Index (MGI) remained within the safe zone (MGI < 1) and the critical zone (1 < MGI < 3), as well as instances when it exceeded the unacceptable range (MGI > 3) over seven years. The WUFI® Pro VTT model denotes these zones using colour-coded indicators: green, yellow, and red. According to the ASHRAE 160 standard, the acceptable performance criterion for mould susceptibility stipulates that MGI should always remain below 3.

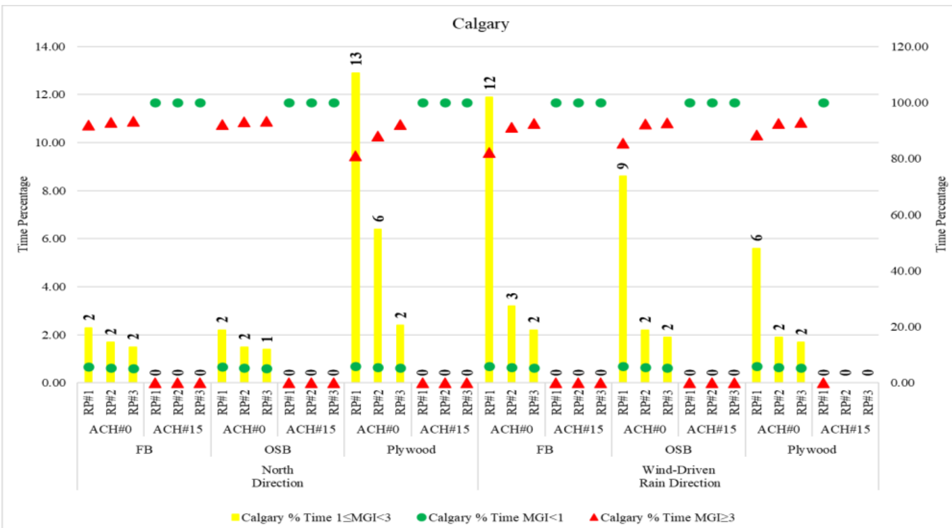


*Figure 3: Calgary - Percentile time Mould Growth Index occurring safe, critical and unacceptable zone throughout the simulation period*

Table 10 shows the yearly occurrence of mould growth index (MGI) values ranging from 1 to 3. Figures 11 to 14 illustrate the percentage of time when the MGI fell within the code indicators for various combinations of direction, material, and conditions across four Canadian cities: Ottawa, Vancouver, Saskatoon, and Calgary. In the northern orientation, the moisture generation index (MGI) consistently exceeded 3 for each sheathing material, except for plywood sheathing located in Vancouver, where the MGI ranged from 40 to 70 percent of the time. Conversely, the 15 ACH effectively mitigated the potential for mould generation, maintaining an MGI of less than one throughout the observation period. When accounting for the ventilation effect within the drainage cavity across the cities assessed in climate zones 7A and 6, the MGI consistently remained below the safe threshold for northern and wind-driven rain orientations. However, when considering the higher rain load rates than ASHRAE 160, precisely at 2% and 3%, the sheathing boards oriented towards wind-driven rain exhibited slower moisture evaporation, resulting in increased susceptibility to mould, with MGI values fluctuating between 1.5 and 3.5

during this period. This finding is particularly significant given the heightened rainfall experienced in coastal climate cities.

To consider the impact of wall orientation, the analysis adhered to ASHRAE 160, which identifies directions with the least solar exposure and the direction of wind-driven rain (Figure 11 – 14). In Saskatoon, the wall orientations were north and northwest-facing, revealing minimal differences in the mould growth index (MGI). With an air changes per hour (ACH) rate of 15, the north-facing wall exhibited a lower MGI than its northwest counterpart. Similar observations were made in Calgary, where no significant differences were noted in the maximum MGI values. Conversely, the southwest-facing brick wall in Ottawa demonstrated a higher MGI than the north-facing wall, a statistically significant difference. Notably, the north orientation in Vancouver showed no mould growth under an ACH of 15, except for the oriented strand board (OSB), which recorded an MGI of 2. In contrast, the southeast-oriented wall exhibited MGI values exceeding three under increased rain exposure. Additionally, it was noted that the performance of fiberboard sheathing was considerably poorer than that of the other two types of sheathing, as OSB has low vapour permeability unless the saturation limit occurs [47].

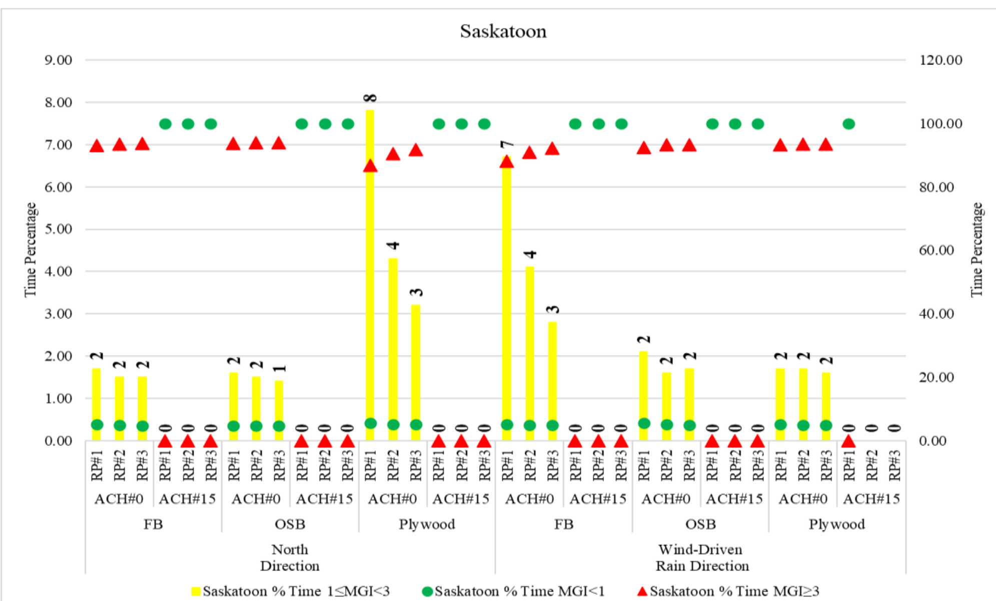


*Figure 4: Saskatoon - Percentile time Mould Growth Index occurring safe, critical and unacceptable zone throughout the simulation period*

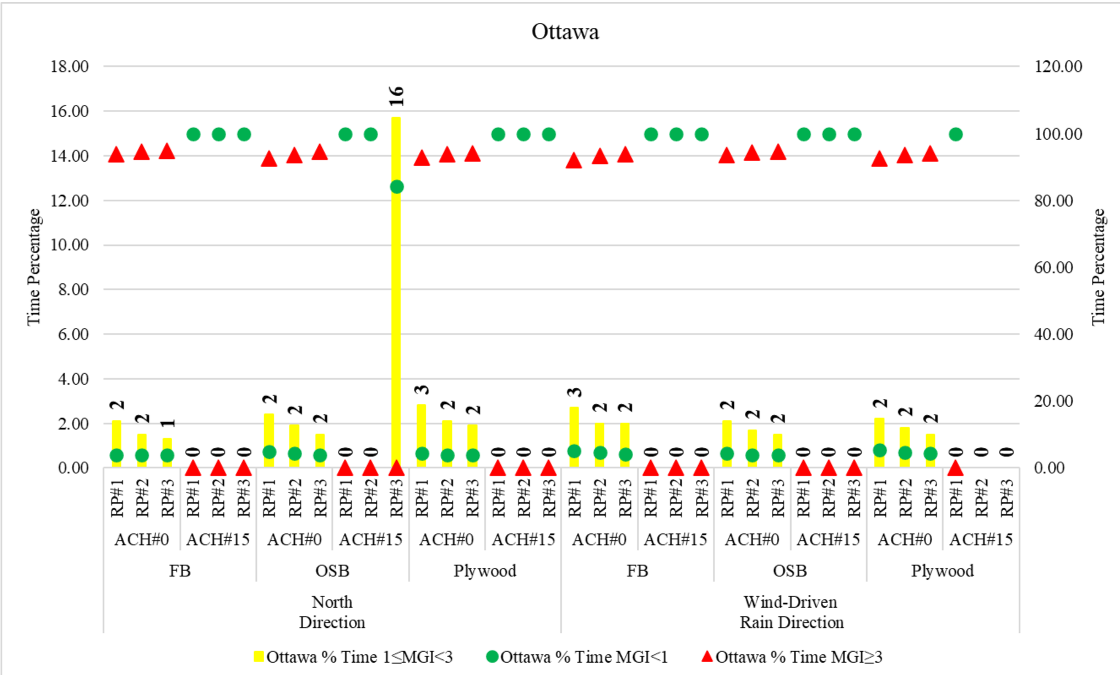


*Figure 5: Ottawa - Percentile time Mould Growth Index occurring safe, critical and unacceptable zone throughout the simulation period*

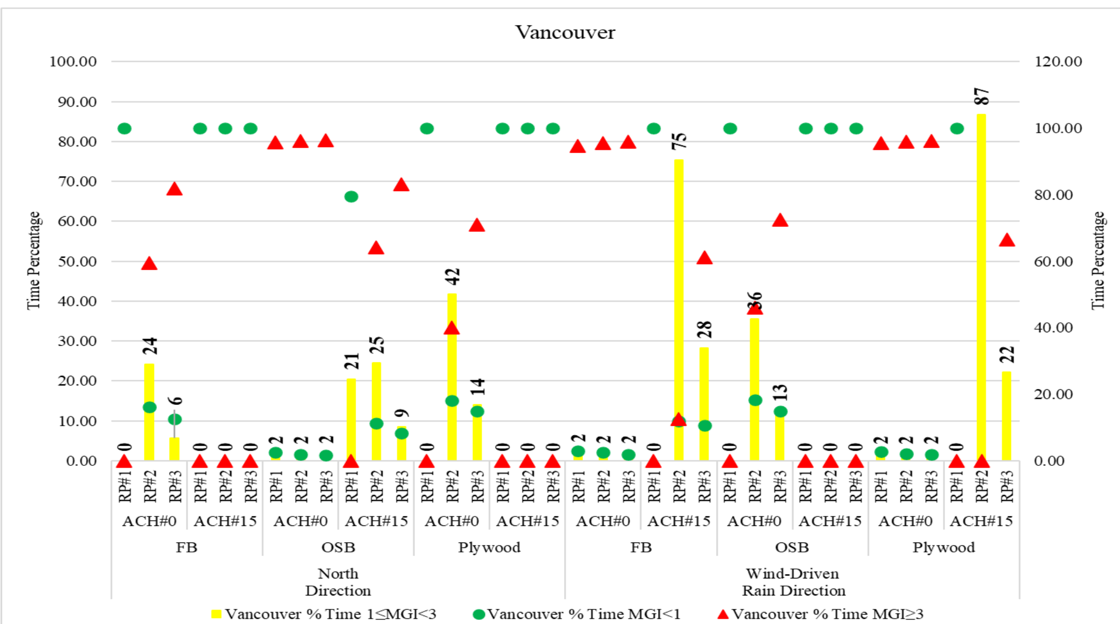


*Figure 6: Vancouver - Percentile time Mould Growth Index occurring safe, critical and unacceptable zone throughout the simulation period*

*Table 10: Percentage of time the MGI remains below 1, between 1 - 3 and above 3 for the tested seven-year simulation period*

| **Direction** | **Material** | **Conditions** | **Ottawa** | | | **Vancouver** | | | **Saskatoon** | | | **Calgary** | | |
|---|---|---|---|---|---|---|---|---|---|---|---|---|---|---|
| | | | **% Time MGI <1** | **% Time 1≤MGI<3** | **% Time MGI ≥3** | **% Time MGI <1** | **% Time 1≤MGI<3** | **% Time MGI ≥3** | **% Time MGI <1** | **% Time 1≤MGI<3** | **% Time MGI ≥3** | **% Time MGI <1** | **% Time 1≤MGI<3** | **% Time MGI ≥3** |
| **North** | **FB** | **ACH#0_RP#1** | 4.00 | 2.10 | 93.90 | 100.00 | 0.00 | 0.00 | 5.30 | 1.70 | 93.00 | 5.70 | 2.30 | 92.00 |
| | | **ACH#0_RP#2** | 3.90 | 1.50 | 94.70 | 16.30 | 24.20 | 59.50 | 4.90 | 1.50 | 93.50 | 5.40 | 1.70 | 93.00 |
| | | **ACH#0_RP#3** | 3.80 | 1.30 | 94.80 | 12.50 | 5.60 | 81.90 | 4.80 | 1.50 | 93.70 | 5.20 | 1.50 | 93.30 |
| | | **ACH#15_RP#1** | 100.00 | 0.00 | 0.00 | 100.00 | 0.00 | 0.00 | 100.00 | 0.00 | 0.00 | 100.00 | 0.00 | 0.00 |
| | | **ACH#15_RP#2** | 100.00 | 0.00 | 0.00 | 100.00 | 0.00 | 0.00 | 100.00 | 0.00 | 0.00 | 100.00 | 0.00 | 0.00 |
| | | **ACH#15_RP#3** | 100.00 | 0.00 | 0.00 | 100.00 | 0.00 | 0.00 | 100.00 | 0.00 | 0.00 | 100.00 | 0.00 | 0.00 |
| | **OSB** | **ACH#0_RP#1** | 5.00 | 2.40 | 92.70 | 2.50 | 1.80 | 95.70 | 4.80 | 1.60 | 93.60 | 5.70 | 2.20 | 92.10 |
| | | **ACH#0_RP#2** | 4.40 | 1.90 | 93.70 | 1.90 | 1.90 | 96.20 | 4.70 | 1.50 | 93.80 | 5.30 | 1.50 | 93.20 |
| | | **ACH#0_RP#3** | 4.00 | 1.50 | 94.50 | 1.60 | 2.00 | 96.40 | 4.70 | 1.40 | 93.80 | 5.20 | 1.40 | 93.40 |
| | | **ACH#15_RP#1** | 100.00 | 0.00 | 0.00 | 79.50 | 20.50 | 0.00 | 100.00 | 0.00 | 0.00 | 100.00 | 0.00 | 0.00 |
| | | **ACH#15_RP#2** | 100.00 | 0.00 | 0.00 | 11.30 | 24.50 | 64.20 | 100.00 | 0.00 | 0.00 | 100.00 | 0.00 | 0.00 |
| | | **ACH#15_RP#3** | 84.30 | 15.70 | 0.00 | 8.30 | 8.60 | 83.10 | 100.00 | 0.00 | 0.00 | 100.00 | 0.00 | 0.00 |
| | **Plywood** | **ACH#0_RP#1** | 4.50 | 2.80 | 92.80 | 100.00 | 0.00 | 0.00 | 5.60 | 7.80 | 86.70 | 5.90 | 12.90 | 81.10 |
| | | **ACH#0_RP#2** | 4.00 | 2.10 | 93.90 | 18.20 | 41.70 | 40.10 | 5.20 | 4.30 | 90.40 | 5.60 | 6.40 | 88.00 |
| | | **ACH#0_RP#3** | 3.90 | 1.90 | 94.20 | 15.00 | 14.00 | 71.00 | 5.10 | 3.20 | 91.70 | 5.40 | 2.40 | 92.20 |
| | | **ACH#15_RP#1** | 100.00 | 0.00 | 0.00 | 100.00 | 0.00 | 0.00 | 100.00 | 0.00 | 0.00 | 100.00 | 0.00 | 0.00 |
| | | **ACH#15_RP#2** | 100.00 | 0.00 | 0.00 | 100.00 | 0.00 | 0.00 | 100.00 | 0.00 | 0.00 | 100.00 | 0.00 | 0.00 |
| | | **ACH#15_RP#3** | 100.00 | 0.00 | 0.00 | 100.00 | 0.00 | 0.00 | 100.00 | 0.00 | 0.00 | 100.00 | 0.00 | 0.00 |
| **WDR** | **FB** | **ACH#0_RP#1** | 5.10 | 2.70 | 92.20 | 2.90 | 2.40 | 94.70 | 5.10 | 6.70 | 88.20 | 5.90 | 11.90 | 82.20 |
| | | **ACH#0_RP#2** | 4.60 | 2.00 | 93.30 | 2.50 | 2.00 | 95.50 | 5.00 | 4.10 | 90.90 | 5.50 | 3.20 | 91.30 |
| | | **ACH#0_RP#3** | 4.20 | 2.00 | 93.80 | 2.00 | 2.10 | 95.90 | 5.00 | 2.80 | 92.20 | 5.40 | 2.20 | 92.50 |
| | | **ACH#15_RP#1** | 100.00 | 0.00 | 0.00 | 100.00 | 0.00 | 0.00 | 100.00 | 0.00 | 0.00 | 100.00 | 0.00 | 0.00 |
| | | **ACH#15_RP#2** | 100.00 | 0.00 | 0.00 | 11.90 | 75.40 | 12.60 | 100.00 | 0.00 | 0.00 | 100.00 | 0.00 | 0.00 |

| | | | | | | | | | | | | | |
|---|---|---|---|---|---|---|---|---|---|---|---|---|---|
| | **ACH#15_RP#3** | 100.00 | 0.00 | 0.00 | 10.60 | 28.30 | 61.10 | 100.00 | 0.00 | 0.00 | 100.00 | 0.00 | 0.00 |
| **OSB** | **ACH#0_RP#1** | 4.30 | 2.10 | 93.60 | 100.00 | 0.00 | 0.00 | 5.60 | 2.10 | 92.30 | 5.90 | 8.60 | 85.50 |
| | **ACH#0_RP#2** | 3.90 | 1.70 | 94.40 | 18.40 | 35.60 | 46.00 | 5.20 | 1.60 | 93.20 | 5.50 | 2.20 | 92.30 |
| | **ACH#0_RP#3** | 3.80 | 1.50 | 94.60 | 15.00 | 12.50 | 72.50 | 5.00 | 1.70 | 93.30 | 5.40 | 1.90 | 92.70 |
| | **ACH#15_RP#1** | 100.00 | 0.00 | 0.00 | 100.00 | 0.00 | 0.00 | 100.00 | 0.00 | 0.00 | 100.00 | 0.00 | 0.00 |
| | **ACH#15_RP#2** | 100.00 | 0.00 | 0.00 | 100.00 | 0.00 | 0.00 | 100.00 | 0.00 | 0.00 | 100.00 | 0.00 | 0.00 |
| | **ACH#15_RP#3** | 100.00 | 0.00 | 0.00 | 100.00 | 0.00 | 0.00 | 100.00 | 0.00 | 0.00 | 100.00 | 0.00 | 0.00 |
| **Plywood** | **ACH#0_RP#1** | 5.30 | 2.20 | 92.50 | 2.70 | 1.80 | 95.50 | 5.10 | 1.70 | 93.20 | 5.90 | 5.60 | 88.50 |
| | **ACH#0_RP#2** | 4.60 | 1.80 | 93.60 | 2.20 | 1.80 | 96.00 | 5.00 | 1.70 | 93.40 | 5.50 | 1.90 | 92.60 |
| | **ACH#0_RP#3** | 4.30 | 1.50 | 94.20 | 1.90 | 1.90 | 96.20 | 4.90 | 1.60 | 93.50 | 5.40 | 1.70 | 92.90 |
| | **ACH#15_RP#1** | 100.00 | 0.00 | 0.00 | 100.00 | 0.00 | 0.00 | 100.00 | 0.00 | 0.00 | 100.00 | 0.00 | 0.00 |
| | **ACH#15_RP#2** | 100.00 | 0.00 | 0.00 | 13.20 | 86.80 | 0.00 | 100.00 | 0.00 | 0.00 | 100.00 | 0.00 | 0.00 |
| | **ACH#15_RP#3** | 100.00 | 0.00 | 0.00 | 11.30 | 22.20 | 66.50 | 100.00 | 0.00 | 0.00 | 100.00 | 0.00 | 0.00 |

# Chapter 5: Conclusion and Recommendations

This study investigated the mould growth potential of three sheathing board materials, i.e., Oriented Strand Board (OSB), Fiberboard (FB) and Plywood (Ply) in a Brick Masonry Wall across different Canadian climate zones (4, 6, and 7A) representing four cities (i) Vancouver, (ii) Ottawa, (iii) Calgary and (iv) Saskatoon. Following the ASHRAE 160-2021, the severity index ($I_{sev}$) method was used to determine a Moisture Reference Year (MRY) representing the severe weather year from 1986 to 2016. A seven-year 1D simulation study was conducted using the WUFI® Pro 6.8 hygrothermal tool and VTT mould index model.

As per ASHRAE 160-2021, the wall was assessed in two distinct directions i.e., (i) wall facing the least solar radiation direction and (ii) wall oriented in the maximum wind-driven rain direction. The mould growth potential, i.e. mould growth index (MGI), was evaluated for three cases of rain penetration (1%, 2%, and 3% of wind-driven rain), and two air change rates (ACH 0 and 15) were considered in the drainage cavity for each case. For this simulation study, the deposition of penetrated rain was taken on the water-resistive barrier.

The results showed that except for 1% wind-driven rain penetration in Vancouver City, the north-oriented wall, i.e., the wall facing the least solar radiation, the mould growth was above the acceptable limit (MGI>3) (rain penetration 2% and 3%), and ventilation was absent, i.e. (ACH 0). In contrast, the results were consistent for Calgary, Ottawa and Saskatoon, considering 1%, 2% and 3% WDR penetration with no ventilation in the drainage cavity. It showed an MGI≥5 for all sheathing material, meaning that more than 50% of the surface was covered by mould. With consideration of ACH 15 in the drainage cavity, the north-oriented wall in Vancouver and Calgary fell under no mould growth criteria (MGI=0); however, Ottawa and Saskatoon observed MGI= 0.5 and MGI 0.8, respectively, corresponds to MGI<1 (i.e., small amount or local growth) as per VTT model when tested for all three WDR penetration rates.

The wall oriented in the maximum WDR direction showed the same results for all four cities, with mould growth of MGI=5.3 considering 1%, 2%, and 3% WDR penetration and no drainage cavity ventilation. In contrast, when ACH 15 was introduced in the drainage cavity, the MGI was noted at 0.1 for Calgary and Saskatoon. The Ottawa location, however, had experienced MGI=1.2 for Fiberboard. Vancouver experiences a higher amount of rain per year, i.e. 1250 mm, for the MRY adopted in this study. The ACH 15 was sufficient to achieve MGI<1 for 1% WDR penetration for all three sheathing boards, but with 2% and 3%, the OSB developed MGI=3.0 and 4, respectively, whereas Plywood had MGI=3.2 and 4.2, respectively. The Fiberboard sheathing mould growth potential was higher for the Vancouver and Ottawa locations when 3% WDR penetration was considered (4.7 and 1.3). However, fiberboard has high water vapour permeability, making it more prone to water being absorbed. This study developed this condition: when more penetrated water is deposited on water resistive barriers (WRB) (i.e. 3%), the fiberboard becomes more saturated, generating adequate conditions for mould development.

Another observation was made to evaluate how long the MGI remained within the safe, critical, and unacceptable range zone over the seven-year simulation period. The VTT model indicates these zones with traffic light signals, i.e., Green, Yellow, and red, as safe, critical, and unacceptable zones. The results showed that when the north-oriented wall was investigated for 1%, 2%, and 3% WDR penetration, showed 80-90% of the time, all three sheathings in all four cities remained in the unacceptable zone (MGI>3) for ACH 0 but remained 100% of the time below MGI<1 when ventilation (ACH 15) was introduced. All cities had the same pattern when considering the maximum wind-driven direction, except for the sheathing boards in Vancouver with ACH15 drainage cavity ventilation. For the 2% WDR penetration, 75% of the time, fiberboard was in the critical zone (i.e., 1 < MGI < 3) and ~90% of the time for 3% WDR penetration. This shows the severity of high rain penetration, keeping sheathing boards more prone to generating high mould growth.

The findings of this study are based on the rain penetration deposited on WRB and emphasize the selection of sheathing material, ventilation rates, and orientation-specific design considerations in mitigating the risks of mould growth and ensuring the long-term durability of wood-frame buildings. The moisture content (MC) is not investigated in this study; however, it serves as a crucial determinant in selecting the air change rate (ACH) necessary to maintain relative humidity (RH) levels in the drainage cavity that mitigate the risk of mould growth and wood decay. Future research endeavours will focus on conducting simulations that explore various wall configurations and materials under differing rain penetrations for all Canadian climate zones. The selection of alternative materials for wall cladding will inevitably influence moisture ingress rates and drainage cavity effectiveness. Additionally, the permeance characteristics of the water-resistant barrier (WRB) and vapour retarder (VRB) significantly impact wall components' wetting and drying dynamics, thereby managing relative humidity values.

# References

[1] "How Weather Changes Contribute to Water Damage | CRS," Canada's Restoration Services. Accessed: Nov. 24, 2024. [Online]. Available: https://www.canadarestorationservices.com/blog/how-weather-changes-contribute-to-water-damage-in-toronto/

[2] "Climate Data to Undertake Hygrothermal and Whole Building Simulations Under Projected Climate Change Influences for 11 Canadian Cities." Accessed: Nov. 18, 2024. [Online]. Available: https://www.mdpi.com/2306-5729/4/2/72

[3] M. Defo, M. A. Lacasse, and L. Wang, "Effects of climate change on the moisture performance and durability of brick veneer walls of wood frame construction in Canada," *J. Phys. Conf. Ser.*, vol. 2069, no. 1, p. 012063, Nov. 2021, doi: 10.1088/1742-6596/2069/1/012063.

[4] A. Gaur and M. Lacasse, "Climate Data to Support the Adaptation of Buildings to Climate Change in Canada," *Data*, vol. 7, no. 4, Art. no. 4, Apr. 2022, doi: 10.3390/data7040042.

[5] S. Nath, "Hygrothermal and mould growth analysis of typical Australian residential wall systems," Thesis, University of Tasmania, 2024. doi: 10.25959/26046721.v2.

[6] Z. Xiao, D. Maurice, L. Wang, and M. A. Lacasse, "Reliability assessment of design reference year for evaluating the impact of climate change on moisture performance of wood frame walls," *Build. Environ.*, vol. 251, p. 111208, Mar. 2024, doi: 10.1016/j.buildenv.2024.111208.

[7] S. Cornick and W. Dalgliesh, "A Moisture Index to Characterize Climates for Building Envelope Design," *J. Build. Phys.*, vol. 27, Oct. 2003, doi: 10.1177/109719603036210.

[8] X. Zhou, D. Derome, and J. Carmeliet, "Robust moisture reference year methodology for hygrothermal simulations," *Build. Environ.*, vol. 110, pp. 23–35, Dec. 2016, doi: 10.1016/j.buildenv.2016.09.021.

[9] "ANSI/ASHRAE 160-2021 - Criteria for Moisture-Control Design Analysis in Buildings." Accessed: Nov. 10, 2024. [Online]. Available: https://webstore.ansi.org/standards/ashrae/ansiashrae1602021?srsltid=AfmBOorJqCpHUeHGWcLV0k4sdLCsljo6bAvQTxnAao7zgd7UAJPMScu4

[10] K. Ghanate, M. Khanverdi, and S. Das, "Wind-driven rainwater penetration through brick veneer with and without surface treatments," *J. Build. Eng.*, vol. 62, p. 105347, Dec. 2022, doi: 10.1016/j.jobe.2022.105347.

[11] "Hygrothermal response of a wood-frame thick-wall assembly to rainwater wetting under future climate scenarios in Canada - Alison Conroy, Phalguni Mukhopadhyaya, Guido Wimmers, 2024." Accessed: Nov. 24, 2024. [Online]. Available: https://journals.sagepub.com/doi/10.1177/17442591241238621

[12] K. Zhang and R. Richman, "Wood sheathing durability from moisture sorption isotherm variability due to age and temperature," *Constr. Build. Mater.*, vol. 273, p. 121672, Mar. 2021, doi: 10.1016/j.conbuildmat.2020.121672.

[13] S. Nath and M. Dewsbury, *The use of an innovative hygrothermal simulation method to develop built fabric recommendations for southern Australia*. University of Tasmania, 2019. Accessed: Nov. 24, 2024. [Online]. Available: https://figshare.utas.edu.au/articles/conference_contribution/The_use_of_an_innovative_hy

grothermal_simulation_method_to_develop_built_fabric_recommendations_for_southern_Australia/23099939/1
[14] "WHO guidelines for indoor air quality : dampness and mould." Accessed: Nov. 24, 2024. [Online]. Available: https://www.who.int/publications/i/item/9789289041683
[15] "Modelling mould growth in domestic environments using relative humidity and temperature - ScienceDirect." Accessed: Nov. 24, 2024. [Online]. Available: https://www.sciencedirect.com/science/article/pii/S0360132321009756
[16] "Evaluation of Moisture Performance of Tall Wood Building Envelope under Climate Change in Different Canadian Climatic Regions." Accessed: Nov. 14, 2024. [Online]. Available: https://www.mdpi.com/1999-4907/14/4/718
[17] "AR5 Synthesis Report: Climate Change 2014 — IPCC." Accessed: Nov. 13, 2024. [Online]. Available: https://www.ipcc.ch/report/ar5/syr/
[18] "A comparison of hygrothermal simulation results derived from four simulation tools - Maurice Defo, Michael Lacasse, Abdelaziz Laouadi, 2022." Accessed: Nov. 12, 2024. [Online]. Available: https://journals.sagepub.com/doi/abs/10.1177/1744259120988760
[19] "Review of rainwater penetration rates in wall assemblies - ScienceDirect." Accessed: Nov. 13, 2024. [Online]. Available: https://www.sciencedirect.com/science/article/pii/S0360132322004498
[20] "A new procedure for selecting moisture reference years for hygrothermal simulations - Zhou - 2016 - Bauphysik - Wiley Online Library." Accessed: Nov. 13, 2024. [Online]. Available: https://onlinelibrary.wiley.com/doi/abs/10.1002/bapi.201610042
[21] C. Aggarwal, M. Defo, T. Moore, M. A. Lacasse, S. Sahyoun, and H. Ge, "Validation of Three Methods of Selecting Moisture Reference Years for Hygrothermal Simulations," *XV Int. Conf. Durab. Build. Mater. Compon. DBMC 2020*, Sep. 2020, doi: 10.23967/dbmc.2020.146.
[22] "Accuracy of using Moisture Reference Years for assessing the Long-Term Moisture Performance of Wall Assemblies - IOPscience." Accessed: Nov. 13, 2024. [Online]. Available: https://iopscience.iop.org/article/10.1088/1742-6596/2654/1/012016
[23] S. Sahyoun, H. Ge, C. Aggarwal, M. Defo, and T. Moore, "Effect of Selected Moisture Reference Year on the Durability Assessment of Wall Assemblies under Future Climates," *XV Int. Conf. Durab. Build. Mater. Compon. EBook Proc.*, 2020, doi: 10.23967/dbmc.2020.056.
[24] G. of C. N. R. C. Canada, "Effects of selected wall orientation on the moisture performance of building envelope - NRC Publications Archive." Accessed: Nov. 11, 2024. [Online]. Available: https://nrc-publications.canada.ca/eng/view/object/?id=5ff6a6ce-ad66-425e-9ff9-9df1557a21dc
[25] C. Aggarwal, M. Defo, H. Ge, and M. A. Lacasse, "Identifying the critical orientation of wood-frame walls in assessing moisture risks using hygrothermal simulation," *J. Phys. Conf. Ser.*, vol. 2069, no. 1, p. 012011, Nov. 2021, doi: 10.1088/1742-6596/2069/1/012011.
[26] G. of C. N. R. C. Canada, "Guideline on design for durability of building envelopes - NRC Publications Archive." Accessed: Nov. 19, 2024. [Online]. Available: https://nrc-publications.canada.ca/eng/view/object/?id=45b6a70c-e5a7-419a-bb1a-4687435c7895
[27] J. Y. Wang *et al.*, "DURABILITY OF MASS TIMBER STRUCTURES: A REVIEW OF THE BIOLOGICAL RISKS," *Wood Fiber Sci.*, pp. 110–127, Aug. 2018.
[28] M. Defo, M. A. Lacasse, and L. Wang, "Effects of climate change on the moisture performance and durability of brick veneer walls of wood frame construction in Canada," *J.*

*Phys. Conf. Ser.*, vol. 2069, no. 1, p. 012063, Nov. 2021, doi: 10.1088/1742-6596/2069/1/012063.

[29] L. Olsson, “Rain intrusion rates at façade details – a summary of results from four laboratory studies,” *Energy Procedia*, vol. 132, pp. 387–392, Oct. 2017, doi: 10.1016/j.egypro.2017.09.639.

[30] M. Defo and M. A. Lacasse, “Effects of Climate Change on the Moisture Performance of Tallwood Building Envelope,” *Buildings*, vol. 11, no. 2, Art. no. 2, Feb. 2021, doi: 10.3390/buildings11020035.

[31] “Advances in hygrothermal building component simulation: modelling moisture sources likely to occur due to rainwater leakage.” Accessed: Nov. 18, 2024. [Online]. Available: https://www.tandfonline.com/doi/epdf/10.1080/19401493.2012.694911?needAccess=true

[32] L. Wang and H. Ge, “Effect of rain leakage on hygrothermal performance of highly insulated wood-framed walls: a stochastic approach,” *Can. J. Civ. Eng.*, vol. 46, no. 11, pp. 979–989, Nov. 2019, doi: 10.1139/cjce-2019-0223.

[33] “(6) A Thermal and moisture property database for common building and insulation materials.” Accessed: Nov. 24, 2024. [Online]. Available: https://www.researchgate.net/publication/44061291_A_Thermal_and_moisture_property_database_for_common_building_and_insulation_materials

[34] “Climate Data to Undertake Hygrothermal and Whole Building Simulations Under Projected Climate Change Influences for 11 Canadian Cities.” Accessed: Nov. 11, 2024. [Online]. Available: https://www.mdpi.com/2306-5729/4/2/72

[35] A. Gaur, “Weather files-building simulations,” Jan. 2019, doi: 10.17605/OSF.IO/UPFXJ.

[36] “Reliability of Moisture Reference Year (MRY) selection methods for hygrothermal performance analysis of wood-frame walls under historical and future climates - ScienceDirect.” Accessed: Nov. 12, 2024. [Online]. Available: https://www.sciencedirect.com/science/article/pii/S0360132321009082

[37] “Controlling Moisture: The Key to Good Buildings | ashrae.org.” Accessed: Nov. 10, 2024. [Online]. Available: https://www.ashrae.org/news/ashraejournal/controlling-moisture-the-key-to-good-buildings

[38] T. Ojanen, H. Viitanen, R. Peuhkuri, K. Lähdesmäki, J. Vinha, and K. Salminen, “Mould growth modeling of building structures using sensitivity classes of materials: Thermal Performance of the Exterior Envelopes of Whole Buildings XI, Buildingx XI Conference,” *Proc. Therm. Perform. Exter. Envel. Whole Build. XI Int. Conf.*, 2010.

[39] “Fraunhofer Institute for building physics | WUFI (en).” Accessed: Nov. 10, 2024. [Online]. Available: https://wufi.de/en/about-us/fraunhofer-institute-for-building-physics/

[40] “WUFI® Pro | WUFI (en).” Accessed: Nov. 10, 2024. [Online]. Available: https://wufi.de/en/software/wufi-pro/

[41] H. Viitanen and T. Ojanen, “Improved model to predict mould growth in building materials: 10th Thermal Performance of the Exterior Envelopes of Whole Buildings Conference,” *Proc. 10th Therm. Perform. Exter. Envel. Whole Build. Conf.*, 2007.

[42] S. Nath, M. Dewsbury, P. Watson, H. Lovell, and H. Kuenzel, *A bio-hygrothermal analysis of typical Australian residential wall systems*. 2020. doi: 10.13140/RG.2.2.32164.91523.

[43] “WUFI® Add-ons | WUFI (en).” Accessed: Nov. 10, 2024. [Online]. Available: https://wufi.de/en/software/wufi-add-ons/

[44] E. Vereecken and D. S. and S. Roels, “A comparison of different mould prediction models,” Jun. 2011, Accessed: Nov. 11, 2024. [Online]. Available: https://www.aivc.org/resource/comparison-different-mould-prediction-models
[45] A. Hukka and H. A. Viitanen, “A mathematical model of mould growth on wooden material,” *Wood Sci. Technol.*, vol. 33, no. 6, pp. 475–485, Dec. 1999, doi: 10.1007/s002260050131.
[46] A. Conroy, P. Mukhopadhyaya, and G. Wimmers, “Hygrothermal response of a wood-frame thick-wall assembly to rainwater wetting under future climate scenarios in Canada,” *J. Build. Phys.*, vol. 47, no. 6, pp. 557–579, May 2024, doi: 10.1177/17442591241238621.
[47] T. Ojanen and J. Ahonen, *Moisture performance properties of exterior sheathing products made of spruce plywood or OSB*. in VTT Working Papers. Espoo: VTT Technical Research Centre of Finland, 2005.

# Appendix

## Appendix 1: WUFI Simulation

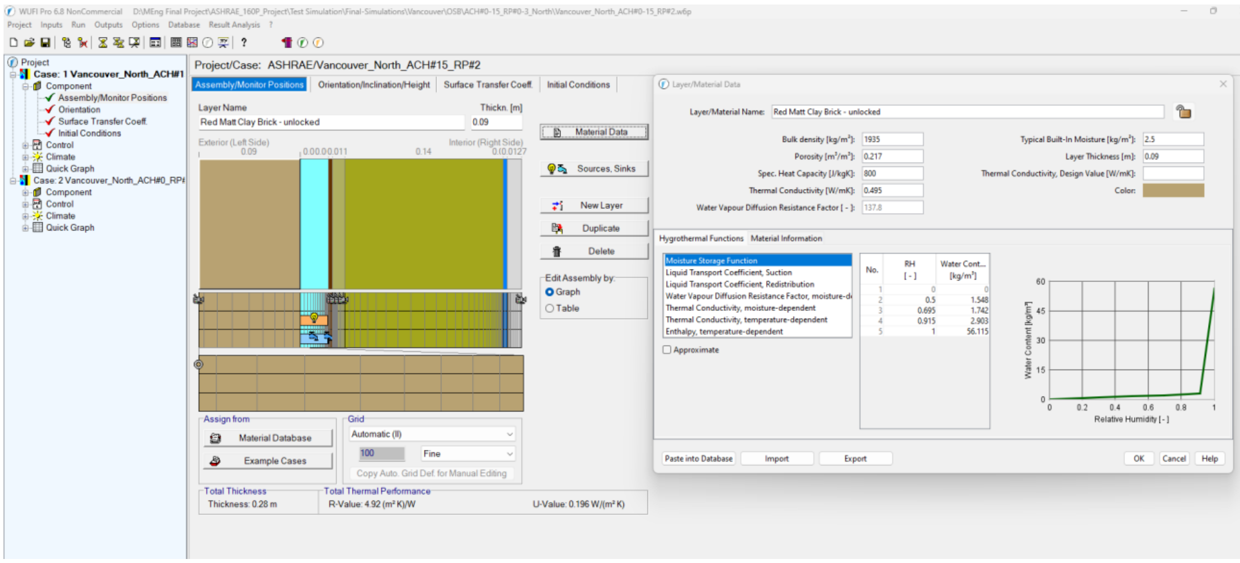


*Figure 75: WUFI material database and properties*

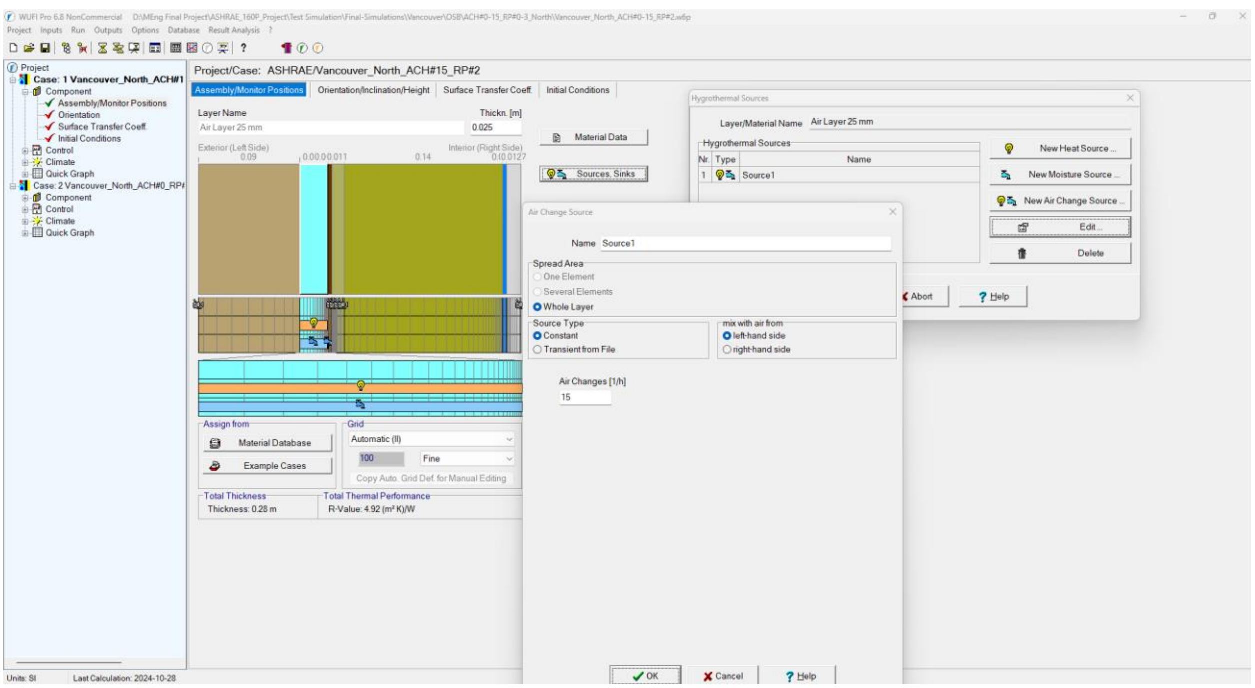


*Figure 86: WUFI simulation Moisture source and Air Change parameter*

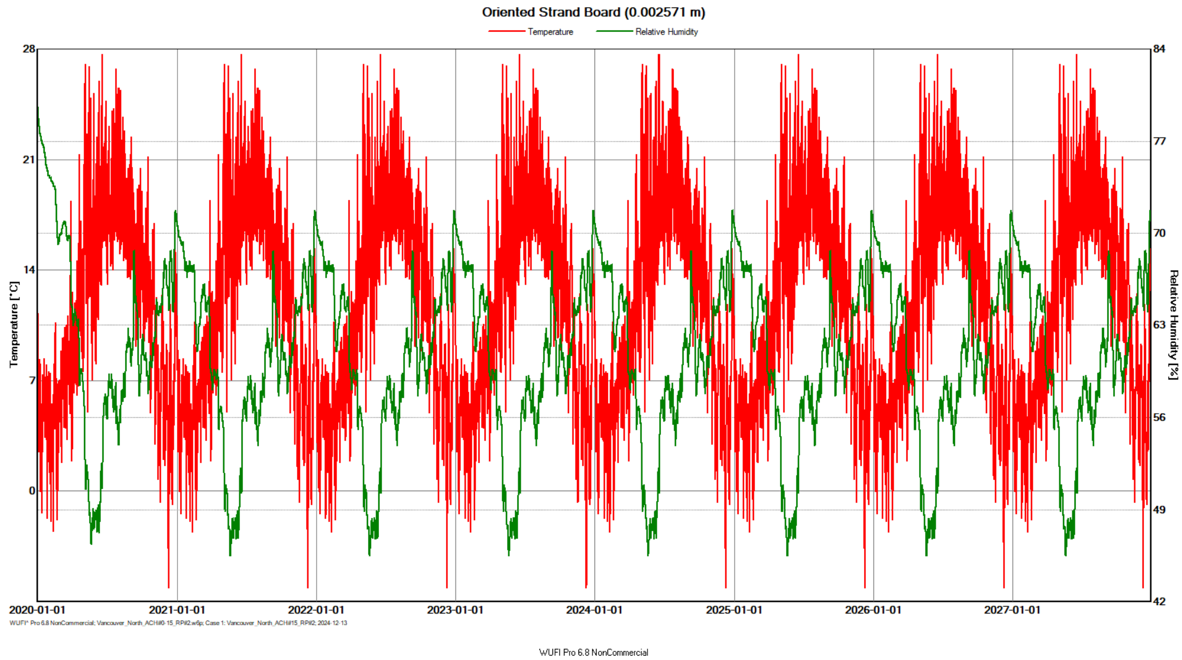


*Figure 17: Temperature and Relative Humidity graph for OSB under ACH15 and Rain penetration 2% for Vancouver location*

# Appendix 2: VTT Simulation

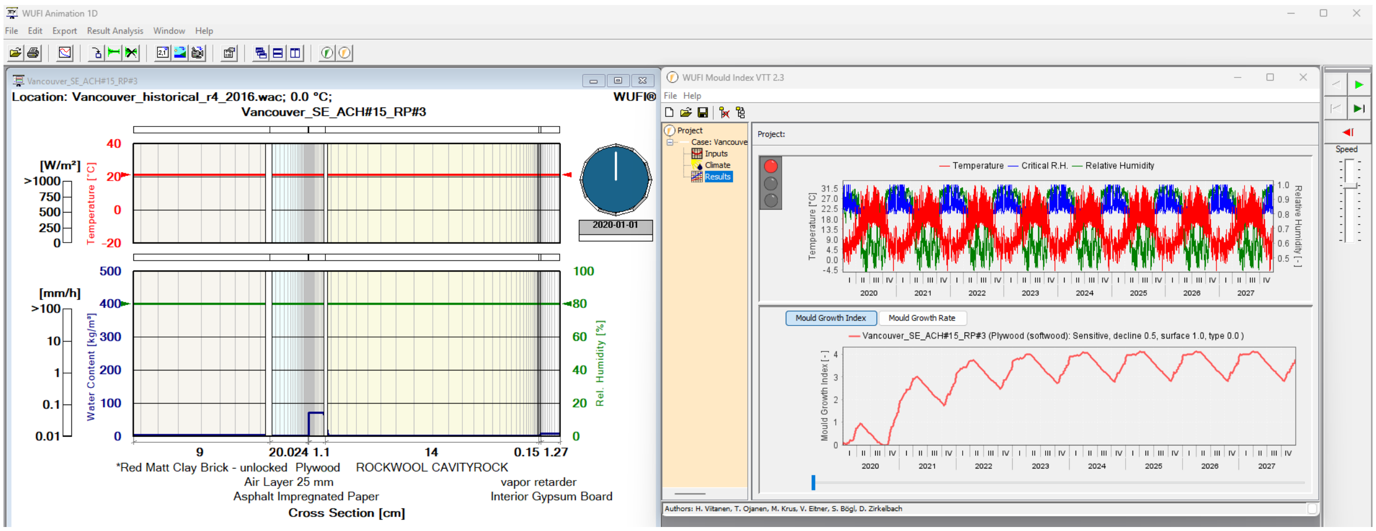


*Figure 18: VTT simulation*

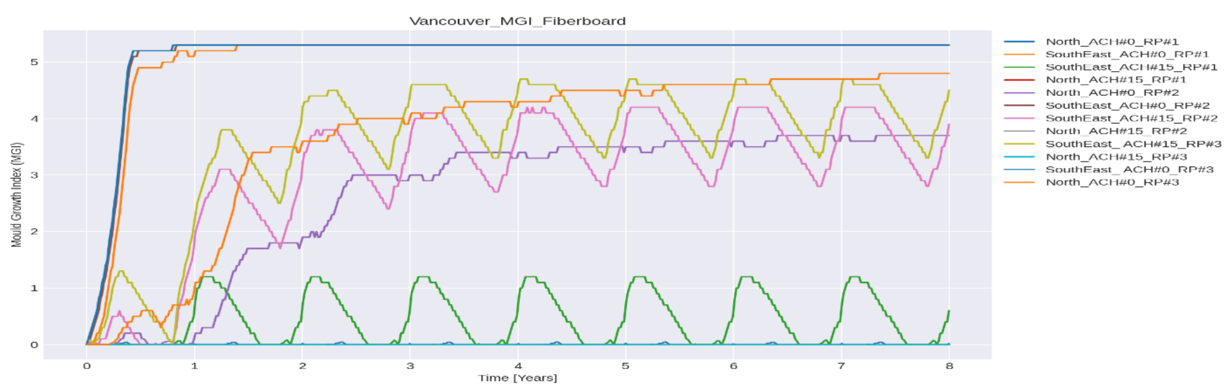


*Figure 19: Mould Growth Index graph of Vancouver location testing Fiberboard Sheathing*

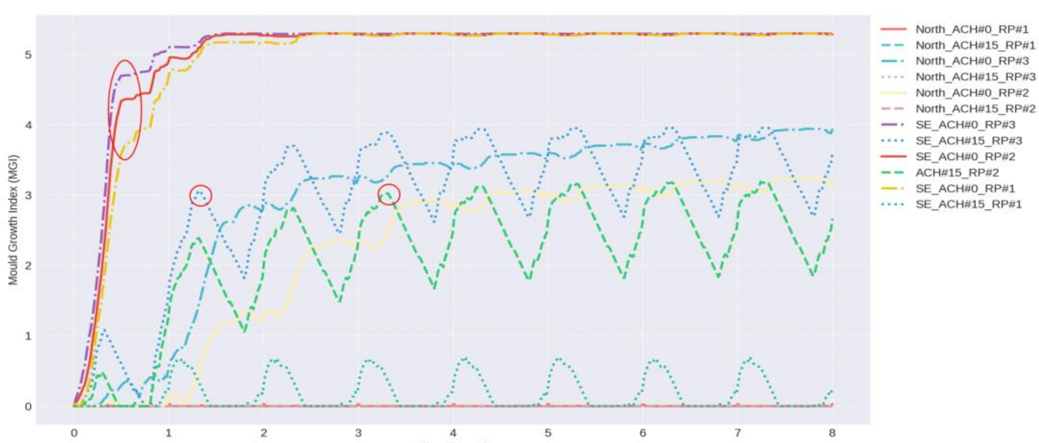


*Figure 20: Mould Growth Index graph of Vancouver location testing OSB Sheathing*